BOUNDARY PARAMETRIZATION AND THE TOPOLOGY OF TILES

SHIGEKI AKIYAMA AND BENOÎT LORIDANT

Abstract. As an application of the boundary parametrization developed in our previous papers, we propose a new method to deduce information on the connected components of the interior of tiles. This gives a systematic way to study the topology of a certain class of self-affine tiles. An example due to Bandt and Gelbrich is examined to prove the efficiency of the method.

§1. Introduction

The topology of self-affine tiles has attracted attention from many researchers (see [Dek82a, Ken92, GH94, LW96b, BG94, BW01]). This is strongly motivated by the construction of Markov partitions (see [Sin68, AW70, Bow70, Bow78, Adl98]). After some pioneering works (see [Dek82b, Ken92]), dual tilings of β-numeration (see [Thu89, Pra92]) and geometric realizations of Pisot substitutions (see [Rau82, AI01]) were systematically studied. The topology of self-affine tiles also shows up in the study of mathematical models of quasicrystals, which initiated a field of research called "mathematics of aperiodic order", going back to Penrose's construction (see [Ken96, Sol97, BM04, KLS15]). It further has connections to theoretical computer science and number theory, and has applications in multiresolution analysis in wavelet expansions (see [GM92, Str93, GH94, Wan02, Cur06]).

We proposed in [AL11] a standard method to parametrize the boundary of self-affine tiles, aiming at giving broad applications of its fine topological study. So far, several applications to prove or disprove the homeomorphy to the closed disk of several classes of tiles have been performed in [AL10] and [Lor16]. Boundary parametrization also gives a way to approximate the boundary by a special substitution. Although such studies have already

appeared in many articles, we stress that our method is a systematic approach to these questions. In this article, we wish to continue this program. We would like to present a new application of our parametrization in order to obtain information on the interior components of non-disklike tiles.

The topology of non-disklike tiles can be very intricate. We can find several, but not many, papers treating this case. Necessary conditions for the disklikeness of the interior components of self-affine tiles with disconnected interior were given in [NT04, NT05]. In [LT08, BLT10], the interior components of the fundamental domain associated with the complex base $-2 + i$ were described in terms of attractors of graph-directed self-similar sets. In [NN03], the cut points of the Heighway dragon were computed and its interior components were shown to be disklike. Moreover, the finitely many shapes of the interior components of the Levy dragon were studied in [BKS02, Als10].

Our idea is to have a close look at the set of identifications appearing in our parametrization. In this paper, we introduce a mild class of identifications which satisfies a *noncrossing* condition. Under this condition and from the computation of the *winding number* of a given point, we can define an *outer identification*. This identification is of special importance, because it produces an interior component by taking a pair of such identifications. Then, from the graph of identifications, we can read the distribution of interior components. The boundary of these is a Jordan closed curve given as explicit continuous images of an interval. An important point is that all of the introduced concepts are checkable by algorithm. Finally, we examine our theory by examples. Basically, we may reproduce similar results to those in [NN03] by our method. As it takes many computations for each example, we illustrate our result by giving a concrete computation of a fractal tile due to Bandt and Gelbrich. We can identify the set of cut points and pick an interior component as the interior of a concrete Jordan closed curve (see Theorem 7). We end this paper by giving some examples where the noncrossing condition is violated.

§2. Fundamental facts on the boundary parametrization

We recall some fundamental facts on our parametrization method for the boundary of self-affine tiles developed in [AL11]. Let A be an *expanding* real $d \times d$ matrix; that is, the eigenvalues of A are greater than 1 in modulus, and $\mathcal{D} \subset \mathbb{R}^d$ a finite set. Then, there is a unique nonempty compact *self-affine*

set $\mathcal{T} = \mathcal{T}(A, \mathcal{D})$ satisfying

$$A\mathcal{T} = \mathcal{T} + \mathcal{D} = \bigcup_{a \in \mathcal{D}} (\mathcal{T} + a)$$

(see [Hut81]). $\mathcal{T}$ is called a self-affine *tile* if it is equal to the closure of its interior. It satisfies the *tiling property* if there is a *tiling set* $\mathcal{J} \subset \mathbb{R}^d$ such that

$$\bigcup_{s \in \mathcal{J}} (\mathcal{T} + s) = \mathbb{R}^d \qquad \text{and} \qquad \lambda_d((\mathcal{T} + s) \cap (\mathcal{T} + s')) = 0 \quad \text{for all } s \neq s' \in \mathcal{J}.$$

Fundamental properties of self-affine tiles were studied in [GH94, LW96a, LW96b]. If A has integer coefficients and $\mathcal{D} \subset \mathbb{Z}^d$ is a complete residue system of $\mathbb{Z}^d$ modulo $A\mathbb{Z}^d$, then $\mathcal{T}$ satisfies the tiling property for some sublattice $\mathcal{J}$ of $\mathbb{Z}^d$ [LW97]. Conditions under which $\mathcal{J} = \mathbb{Z}^d$ are investigated in [GH94, Vin00]. We then say that $\mathcal{T}$ is an *integral self-affine $\mathbb{Z}^d$-tile*.

A powerful tool in the study of an integral self-affine $\mathbb{Z}^d$-tile $\mathcal{T} = \mathcal{T}(A, \mathcal{D})$ is the *boundary automaton*. For a set $U \subset \mathbb{Z}^d$, we define the following automaton $G(U)$.

- The set of vertices is U.
- There is an edge $s \xrightarrow{a|a'} s'$ $(s, s' \in U, a, a' \in \mathcal{D})$ if and only if $As + a' = s + a$. We may simply write $s \xrightarrow{a} s' \in G(U)$. (This determines a' uniquely.)

Taking for U the set

$$\mathcal{S} := \{s \in \mathbb{Z}^d \backslash \{0\}; \mathcal{T} \cap (\mathcal{T} + s) \neq \emptyset\},$$

we obtain the boundary automaton $G(\mathcal{S})$. By compactness of $\mathcal{T}$, $\mathcal{S}$ is finite. There exist algorithms to compute $G(\mathcal{S})$ from the data $(A, \mathcal{D})$ (see, for example, [ST03]). This automaton gives a way to express the boundary as the attractor of a graph-directed iterated function system (GIFS) (see [MW88]).

PROPOSITION 2.1. *Given an integral self-affine $\mathbb{Z}^d$-tile $\mathcal{T} = \mathcal{T}(A, \mathcal{D})$ and its boundary automaton $G(\mathcal{S})$, the boundary $\partial\mathcal{T}$ satisfies*

$$\partial\mathcal{T} = \bigcup_{s \in \mathcal{S}} B_s,$$

where for all $s \in \mathcal{S}$,

$$B_s = \bigcup_{s \xrightarrow{a} s' \in G(\mathcal{S})} A^{-1}(B_{s'} + a).$$

Moreover, $B_s = \mathcal{T} \cap (\mathcal{T} + s)$, and for two sequences of digits $(a_i)_{i \geqslant 1}$, (a'_i), we have

$$\sum_{n \geqslant 1} A^{-n} a_n = s + \sum_{n \geqslant 1} A^{-n} a'_n$$

if and only if there is an infinite walk

$$s \xrightarrow{a_1|a'_1} s_1 \xrightarrow{a_2|a'_2} \cdots \in G(\mathcal{S}).$$

Usually, the boundary automaton contains a great deal of redundant information, due to the existence of multiple points in the tiling. This often makes $G(\mathcal{S})$ too large to perform our parametrization method. We make the following assumptions.

Assumption 1. There exists a set $\mathcal{R} \subset \mathcal{S}$ such that the following holds.

- $G(\mathcal{R})$ is strongly connected; that is, its incidence matrix

$$\mathbf{C} = (c_{s,s'})_{s,s' \in \mathcal{R}} \quad \text{with } c_{s,s'} = \#\{s' \to s \in G(\mathcal{R})\}$$

  is irreducible.
- $G(\mathcal{R})$ is a GIFS for $\partial \mathcal{T}$; that is,

$$(2.1) \qquad \begin{cases} \partial \mathcal{T} = \bigcup_{s \in \mathcal{R}} K_s, \\ K_s = \bigcup_{s \xrightarrow{a} s' \in G(\mathcal{R})} A^{-1}(K_{s'} + a) \quad (s \in \mathcal{R}). \end{cases}$$

In this case, $K_s \subset \mathcal{T} \cap (\mathcal{T} + s)$.

REMARK 2.2. In many applications, a subset of the *contact set* constructed in [GH94]) can be used as a good candidate for such a smaller set $\mathcal{R} \subset \mathcal{S}$ and leads to the *contact automaton*. If A is a similarity matrix of factor λ and β is the largest root of the incidence matrix of the contact automaton, it is well known (see [DKV00]) that the Hausdorff dimension of $\partial \mathcal{T}$ is given by the formula

$$\dim_{\mathrm{H}} \partial \mathcal{T} = \frac{\log \beta}{\log \lambda}.$$

As $G(\mathcal{R})$ is strongly connected, there is a strictly positive left eigenvector $(u_s)_{s \in \mathcal{R}}$ of length 1 associated to the Perron–Frobenius eigenvalue β of

its incidence matrix. The parametrization $C : [0,1] \to \partial \mathcal{T}$ is obtained by subdividing the interval $[0,1]$ proportionally to the automaton $G(\mathcal{R})$. In particular, a subinterval of length u_s is mapped to K_s for each $s \in \mathcal{R}$. To this effect, we order the boundary pieces K_s around the boundary, as well as the subpieces $A^{-1}(K_{s'} + a)$ constituting K_s.

Under the above Assumption 1, let $p = |\mathcal{R}|$, and let $\mathcal{R} =: \{s^1, \ldots, s^p\}$. This orders the states of $G(\mathcal{R})$ arbitrarily from 1 to p. Similarly, for each $i \in \{1, \ldots, p\}$, we order all of the edges starting from s^i arbitrarily, from $\mathbf{1}$ to $\mathbf{o_m}$. Here, $\mathbf{o_m}$ is the total number of edges starting from s^i, without reference to i for the sake of simplicity. We call the resulting automaton an *ordered extension* of $G(\mathcal{R})$ and write it as $G(\mathcal{R})^o$. In other words, the mapping

$$G(\mathcal{R})^o \to G(\mathcal{R})$$
$$i \xrightarrow{a|a'||\mathbf{o}} j =: (i; \mathbf{o}) \mapsto s^i \xrightarrow{a|a'} s^j$$

is a bijection. We can extend this mapping to the walks of arbitrary length in $G(\mathcal{R})$ (possibly infinite walks),

$$G(\mathcal{R})^o \to G(\mathcal{R}),$$
$$(i; \mathbf{o_1}, \mathbf{o_2}, \ldots) \mapsto s^i \xrightarrow{a_1} s^{j_1} \xrightarrow{a_2} s^{j_2} \ldots,$$

whenever $i \xrightarrow{a_1|a_1'||\mathbf{o_1}} j_1 \xrightarrow{a_2|a_2'||\mathbf{o_2}} j_2 \ldots \in G(\mathcal{R})^o$. Finally, we define the natural onto mapping,

$$\psi : G(\mathcal{R})^o \to \partial \mathcal{T},$$
$$v \mapsto \sum_{n \geqslant 1} A^{-n} a_n,$$

whenever $v : s \xrightarrow{a_1|a_1'||\mathbf{o_1}} s_1 \xrightarrow{a_2|a_2'||\mathbf{o_2}} s_2 \ldots$ is an infinite walk in $G(\mathcal{R})^o$. The automaton $G(\mathcal{R})^o$ induces a β-number system $\phi^{(1)} : [0,1] \to G(\mathcal{R})^o$ of Dumont–Thomas type [DT89]. The following compatibility conditions ensure the continuity of the parametrization.

DEFINITION 2.3. (Compatibility conditions) We call $G(\mathcal{R})^o$ a *compatible ordered extension* of $G(\mathcal{R})$ if

$$(2.2) \qquad \psi(i; \overline{\mathbf{o_m}}) = \psi(i+1; \overline{\mathbf{1}}) \quad (1 \leqslant i \leqslant p-1),$$

$$(2.3) \qquad \psi(p; \overline{\mathbf{o_m}}) = \psi(1; \overline{\mathbf{1}}),$$

$$(2.4) \qquad \psi(i; \mathbf{o}, \overline{\mathbf{o_m}}) = \psi(i; \mathbf{o+1}, \overline{\mathbf{1}}) \quad (1 \leqslant i \leqslant p, \mathbf{1} \leqslant \mathbf{o} < \mathbf{o_m}).$$

We denote by $\overline{\mathbf{o}}$ the infinite repetition of $\mathbf{o}, \mathbf{o}, \dots$. Whether an ordered extension is compatible or not can be checked algorithmically. In [AL11], we proved the following result by taking $C := \Psi \circ \phi^{(1)}$.

THEOREM 2.4. [AL11, Theorem 1] *Let $\mathcal{T} = \mathcal{T}(A, \mathcal{D})$ be an integral self-affine $\mathbb{Z}^d$-tile, and let the set $\mathcal{R}$ satisfy the above assumptions. Let β be the Perron–Frobenius eigenvalue of the incidence matrix of $G(\mathcal{R})$. Moreover, suppose that there exists a compatible ordered extension of $G(\mathcal{R})$. Then, there exist a Hölder continuous onto mapping $C : [0, 1] \to \partial T$ with $C(0) = C(1)$ and a sequence $(\Delta_n)_{n \geqslant 0}$ of polygonal curves with the following properties.*

(1) $\lim_{n \to \infty} \Delta_n = \partial T$ *(Hausdorff metric)*.
(2) *Denote by V_n the set of vertices of Δ_n. For all $n \in \mathbb{N}$, $V_n \subset V_{n+1} \subset C(\mathbb{Q}(\beta) \cap [0, 1])$ (i.e., the vertices have $\mathbb{Q}(\beta)$-addresses in the parametrization).*

REMARK 2.5. The polygonal approximations Δ_n appear in a natural way together with the parametrization. Δ_0 is obtained by joining by straight line segments the points

$$\psi(1; \overline{\mathbf{1}}), \psi(2; \overline{\mathbf{1}}), \dots, \psi(p; \overline{\mathbf{1}}), \psi(1; \overline{\mathbf{1}})$$

in this order. In general, let $w_1^{(n)}, \dots, w_{m_n}^{(n)}$ be the walks of length n in the automaton $G(\mathcal{R})^o$, written in the lexicographical order, from $(1; \underbrace{\mathbf{1}, \dots, \mathbf{1}}_{n \text{ times}})$ to $(p; \underbrace{\mathbf{o_m}, \dots, \mathbf{o_m}}_{n \text{ times}})$. Let us denote by $(i; \mathbf{o_1}, \dots, \mathbf{o_n}) \& \overline{\mathbf{1}}$ the concatenated walk $(i; \mathbf{o_1}, \dots, \mathbf{o_n}, \overline{\mathbf{1}})$. Then, Δ_n is obtained by joining by straight line segments the points

$$\psi(w_1^{(n)} \& \overline{\mathbf{1}}), \dots, \psi(w_{m_n}^{(n)} \& \overline{\mathbf{1}}), \psi(w_1^{(n)} \& \overline{\mathbf{1}})$$

in this order. Each vertex of Δ_n corresponds to an infinite walk ending up in a cycle of $G(\mathcal{R})$. Thus, these are images of fixed points of contractions,

$$(f_{a_1} \circ \dots \circ f_{a_l}) \left(\text{Fix}(f_{a_{l+1}} \circ \dots \circ f_{a_{l+n}}) \right),$$

where $f_a(x) := A^{-1}(x + a)$ for each $a \in \mathcal{D}$.

§3. Winding number

The *winding number* is defined for a simple closed curve J and a point $x_0 \notin J$ in [Ale98, Part 1, Chapter II] to show Jordan's curve theorem.

Assumption 2. We suppose that in each step of the approximation, our standard parametrization gives a *simple* closed polygonal curve Δ_n.

This was shown to be the case for many examples, as in [AL11] or at the end of this article. Then, we can employ the same definition

$$W(x_0, \partial\mathcal{T}) = \frac{1}{2\pi} \int_{\partial\mathcal{T}} d(angle(x - x_0))$$

for the winding number of x_0 around $J = \partial\mathcal{T}$, where the right-hand side is the limit as the broken lines Δ_n converge to the boundary in the Hausdorff metric. Since $\{x_0\}$ and $\partial\mathcal{T}$ are closed sets, they are separated by a positive distance if $x_0 \notin \partial\mathcal{T}$. Therefore, if the approximation of $\partial\mathcal{T}$ by broken lines is fine enough, then $W(x_0, \partial\mathcal{T})$ is computed as a finite sum and the above $W(x_0, \partial\mathcal{T})$ is well-defined. Clearly, $W(x_0, \partial\mathcal{T}) = 1$ (resp. 0) if x_0 is an inner point of $\mathcal{T}$ (resp. outside of $\mathcal{T}$).

Using the *encircling method* introduced by Akiyama and Sadahiro in [AS98], we can give a covering of $\partial\mathcal{T}$ by a finite number of disks whose union does not contain x_0. By this method, we can deduce how many steps of approximation by broken lines are necessary to compute the winding number $W(x_0, \partial\mathcal{T})$ when $x_0 \notin \partial\mathcal{T}$. This gives an easy application of the boundary parametrization, described by the following theorem. Given a self-affine tile $\mathcal{T}$ satisfying Assumptions 1 and 2, and $x_0 \in \partial\mathcal{T}$, a computer calculation can decide whether x_0 is an inner point of $\mathcal{T}$ or of $\mathbb{R}^2 \backslash \mathcal{T}$.

THEOREM 1. *For a given point $x_0 \notin \partial T$, there is an algorithm to tell whether x_0 is an inner point of $\mathcal{T}$ or of $\mathbb{R}^2 \backslash \mathcal{T}$.*

Proof. Since A is an expanding matrix, we can find $k > 0$ and $0 < \lambda < 1$ such that $A^{-k}\mathbb{D}(0; 1) \subset \lambda\mathbb{D}(0; 1)$. Here, $\mathbb{D}(0; 1)$ denotes the closed disk of center 0 and radius 1. For the sake of simplicity, we write the proof under the assumption that $k = 1$. If $k > 1$, the argument below remains true by taking $A' := A^k$ and $\mathcal{D}' = \mathcal{D} + A\mathcal{D} + \cdots + A^{k-1}\mathcal{D}$. Note that the associated tile $\mathcal{T}'$ satisfies $\mathcal{T}' = \mathcal{T}$.

Since $\mathcal{T}$ is compact, there is $r > 0$ such that $\mathcal{T} \subset \mathbb{D}(0; r) =: \mathbb{D}_r$. In particular, for all $m \geqslant 0$,

$$A^{-m}\mathcal{T} \subset A^{-m}\mathbb{D}_r \subset \lambda^m\mathbb{D}_r,$$

the latter set being a closed disk of diameter $2r\lambda^m$. We show that $W(x_0, \Delta_m) = W(x_0, \partial\mathcal{T})$ as soon as m satisfies

$$2r\lambda^m < \text{dist}(x_0, \partial\mathcal{T}).$$

Indeed, iterating (2.1), for all $m \geqslant 1$, we can write

$$(3.1) \begin{cases} \partial\mathcal{T} = \bigcup_{s \in \mathcal{R}} K_s, \\ K_s = \bigcup_{s \xrightarrow{a_1} s_1 \xrightarrow{a_2} \cdots \xrightarrow{a_m} s_m \in G(\mathcal{R})} \left(A^{-m} K_{s_m} + A^{-1}a_1 + \cdots + A^{-m}a_m \right) \quad (s \in \mathcal{R}). \end{cases}$$

Using that $K_s \subset \mathcal{T} \subset \mathbb{D}_r$ for all $s \in \mathcal{R}$, we obtain for all $m \geqslant 1$ that

$$\partial\mathcal{T} \subset F_m := \bigcup_{s \in \mathcal{R}} \bigcup_{s \xrightarrow{a_1} s_1 \xrightarrow{a_2} \cdots \xrightarrow{a_m} s_m \in G(\mathcal{R})} \left(\lambda^m \mathbb{D}_r + A^{-1}a_1 + \cdots + A^{-m}a_m \right).$$

Therefore,

$$\begin{aligned} \text{dist}\left(x_0, F_m\right) = \text{dist}&\left(x_0, \bigcup_{s \in \mathcal{R}} \bigcup_{s \xrightarrow{a_1} s_1 \xrightarrow{a_2} \cdots \xrightarrow{a_m} s_m \in G(\mathcal{R})} \right. \\ &\left. \times \left(\lambda^m \mathbb{D}_r + A^{-1}a_1 + \cdots + A^{-m}a_m \right) \right) \\ = \min &\left\{ \text{dist}\left(x_0, \lambda^m \mathbb{D}_r + A^{-1}a_1 + \cdots + A^{-m}a_m\right) ; \right. \\ &\left. s \in \mathcal{R}, s \xrightarrow{a_1} s_1 \xrightarrow{a_2} \cdots \xrightarrow{a_m} s_m \in G(\mathcal{R}) \right\} \\ \geqslant\ & \text{dist}(x_0, \partial\mathcal{T}) - \text{diam}(\lambda^m \mathbb{D}_r) = \text{dist}(x_0, \partial\mathcal{T}) - 2r\lambda^m. \end{aligned}$$

The inequality is justified as follows. Each disk appearing in the lower union of (3.1) intersects ∂T, because

$$(3.2) \quad A^{-1}a_1 + \cdots + A^{-m}a_m + A^{-m}\mathcal{T} \subset A^{-1}a_1 + \cdots + A^{-m}a_m + \lambda^m \mathbb{D}_r$$

and $(a_1, \ldots, a_m)$ is a sequence of digits labeling a walk in $G(\mathcal{R})$.

By this inequality, the assumption that $x_0 \notin \partial\mathcal{T}$ ensures the existence of $m \geqslant 1$ such that $\mathrm{dist}(x_0, F_m) > 0$. Let $N \geqslant 1$ be the least integer such that $x_0 \notin F_N$.

Now, let $w := w_k^{(N)} : s \xrightarrow{a_1} s_1 \xrightarrow{a_2} \cdots \xrightarrow{a_N} s_N$ be a walk of length N in $G(\mathcal{R})$ for some $1 \leqslant k \leqslant m_N$, as defined in Remark 2.5. The associated segment

$$\left[\psi(P(w\&\overline{\mathbf{1}})), \psi(P(w\&\overline{\mathbf{o_m}})) \right] = \left[\psi(P(w_k^{(N)}\&\overline{\mathbf{1}})), \psi(P(w_{k+1}^{(N)}\&\overline{\mathbf{1}})) \right] \subset \Delta_N$$

is a subset of the disk $F_w := \lambda^N \mathbb{D}_r + A^{-1}a_1 + \cdots + A^{-N}a_N$, because its endpoints belong to this convex set by (3.2). (We define $w_{m_N+1}^{(N)} := w_1^{(N)}$.) Since these segments build up Δ_N, we obtain that $\Delta_N \subset F_N$. In particular,

$$\mathrm{dist}(x_0, \Delta_N) > 0.$$

Moreover, for any $w := s \xrightarrow{a_1} s_1 \xrightarrow{a_2} \cdots \xrightarrow{a_N} s_N$ as above and any $w' := s \xrightarrow{a_1} s_1 \xrightarrow{a_2} \cdots \xrightarrow{a_n} s_n$ with $n \geqslant N$ (that is, w' starts like w), the corresponding segment

$$\left[\psi(P(w'\&\overline{\mathbf{1}})), \psi(P(w'\&\overline{\mathbf{o_m}})) \right] \subset \Delta_N$$

remains in the disk F_w, again by (3.2). It follows that the simple closed curve Δ_n can be obtained by continuous deformation (homotopy) of Δ_N inside F_N. This homotopy fixes the vertices of Δ_N.

We conclude that for all $n \geqslant N$,

$$W(x_0, \Delta_n) = W(x_0, \Delta_N) = W(x_0, \partial\mathcal{T}).$$

This gives an algorithm to compute $W(x_0, \partial\mathcal{T})$ and decide whether x_0 is an inner point of $\mathcal{T}$ or of $\mathbb{R}\backslash\mathcal{T}$.

Indeed, we can check by computer whether $x_0 \in F_m$ or $x_0 \notin F_m$ for $m = 1, 2, \ldots$. Note that suitable λ and r are computable from the matrix A and the digit set $\mathcal{D}$. The least $m \geqslant 1$ such that $x_0 \notin F_m$ defines N. Then, we can compute the winding number $W(x_0, \Delta_N)$. Δ_N is a simple closed polygonal curve, whose vertices are computable because they are images of fixed points of contractions,

$$(f_{a_1} \circ \ldots \circ f_{a_l})\left(\mathrm{Fix}(f_{a_{l+1}} \circ \ldots \circ f_{a_{l+n}})\right),$$

where $f_a(x) := A^{-1}(x + a)$ for each $a \in \mathcal{D}$ (see Remark 2.5). The value (0 or 1) of this winding number indicates whether x_0 is an inner point of $\mathcal{T}$ or of its complement. □

Note that without the knowledge of $x_0 \notin \partial\mathcal{T}$, there is no algorithm to tell whether a point lies in $\mathcal{T}$ or not [Dub93].

§4. Outer identifications

Let $C : [0, 1] \to \partial\mathcal{T}$ be the parametrization with $C(0) = C(1)$.

DEFINITION 4.1. A pair (a, b) with $0 < a < b < 1$ is an *identification* if $C(a) = C(b)$. Two identifications (a, b) and (c, d) are *crossing* if either $a < c < b < d$ or $c < a < d < b$ holds.

In this paper, we restrict to the case where no pairs of identifications are crossing. This is not the general case, as we mention in Section 7.

In order to classify the identifications, we need to compute the winding number of points with respect to subsets of the boundary $\partial\mathcal{T}$. We denote by $(\Delta_n)_{n \geqslant 0}$ the sequence of simple closed polygonal curves approximating $\partial\mathcal{T}$. For each n, the vertices of Δ_n are points $C(t_k^{(n)}) \in \partial\mathcal{T}$, $k \in \{0, \dots, m_n\}$, where $0 = t_0^{(n)} < t_1^{(n)} < \cdots < t_{m_n}^{(n)} = 1$. For an identification (a, b), we define

$$a_n := \max\{t_k^{(n)}; t_k^{(n)} \leqslant a\}, \quad b_n := \min\{t_k^{(n)}; t_k^{(n)} \geqslant b\},$$

```
            →              ←
 ├──────────┼──┼───────┼───┼──────────┤
 0         a_n  a       b   b_n        1
```
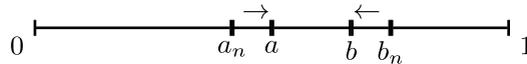
Note that $(a_n)_{n \geqslant 0}$ is increasing and converges to a, whereas $(b_n)_{n \geqslant 0}$ is decreasing and converges to b. Let us consider

(i) $C_n(a_n, b_n)$, the closed polygonal curve obtained by joining the points $C(t_k^{(n)})$ consecutively for $a_n \leqslant t_k^{(n)} \leqslant b_n$, and adding the segment $[C(b_n), C(a_n)]$;

(ii) $D_n(a_n, b_n)$, the closed polygonal curve

$$D_n(a_n, b_n) = (\Delta_n \backslash C_n(a_n, b_n)) \cup [C(b_n), C(a_n)].$$

The curve $C_n(a_n, b_n) \backslash\,]C(b_n), C(a_n)[$ is a subset of Δ_n; thus, $C_n(a_n, b_n)$ may intersect itself only along the added segment $[C(b_n), C(a_n)]$. This also holds for $D_n(a_n, b_n)$. Moreover, in the Hausdorff metric, $(C_n(a_n, b_n))_{n \geqslant 0}$ converges to $C([a, b])$, while $(D_n(a_n, b_n))_{n \geqslant 0}$ converges to $C([0, a]) \cup C([b, 1])$.

LEMMA 4.2. *Let* $y \in \mathbb{R}^2 \backslash C([a, b])$. *Then, the sequence* $(W(y, C_n(a_n, b_n)))_{n \geqslant 0}$ *is eventually well-defined and constant of value either 0 or 1.*

Proof. We denote by $\mathrm{dist}_H(A, B)$ the Hausdorff distance between two nonempty compact sets A, B of $\mathbb{R}^2$. Let $y \in \mathbb{R}^2 \backslash C([a, b])$, and let $\epsilon > 0$, such that $\mathrm{dist}_H(\{y\}, C([a, b])) > \epsilon$. Let us choose integers as follows.

- N_1 such that the Hausdorff distances

$$\mathrm{dist}_H(\Delta_n, \partial\mathcal{T}), \quad \mathrm{dist}_H(C_n(a_n, b_n), C([a, b])),$$

$$\mathrm{dist}_H(D_n(a_n, b_n), C([0, a]) \cup C([b, 1]))$$

  are at most $\epsilon/4$ for all $n \geqslant N_1$.
- N_2 such that for all $n \geqslant N_2$, the points $C(a_n)$ and $C(b_n)$ belong to the disk $\mathbb{D}(C(a); \epsilon/4)$ of center $C(a) = C(b)$ and radius $\epsilon/4$.

Let $N := \max\{N_1, N_2\}$. Note that, by assumption, y belongs to $\mathbb{R}^2 \backslash C_n(a_n, b_n)$ for all $n \geqslant N$.

We now fix $n \geqslant N$. We show that $C_{n+1}(a_{n+1}, b_{n+1})$ is obtained from $C_n(a_n, b_n)$ by continuous deformation (homotopy) avoiding y. Indeed, the simple polygonal arcs

$$C_n(a_n, b_n)\backslash]C(b_n), C(a_n)[\qquad \text{and} \qquad C_{n+1}(a_{n+1}, b_{n+1})\backslash]C(b_{n+1}), C(a_{n+1})[$$

are at most at $\epsilon/2$-Hausdorff distance from each other; thus, there is a homotopy between these arcs that does not intersect the disk $\mathbb{D}(y; \epsilon/4)$. Moreover, there exists a homotopy between the segments

$$[C(b_n), C(a_n)] \qquad \text{and} \qquad [C(b_{n+1}), C(a_{n+1})]$$

inside the disk $\mathbb{D}(C(a); \epsilon/2)$, thus avoiding the disk $\mathbb{D}(y; \epsilon/4)$.

We infer the existence of a homotopy between the polygonal curves $C_n(a_n, b_n)$ and $C_{n+1}(a_{n+1}, b_{n+1})$ that avoids the point y. Therefore, the winding number remains constant:

$$W(y, C_n(a_n, b_n)) = W(y, C_{n+1}(a_{n+1}, b_{n+1})),$$

for all $n \geqslant N$.

We finally show that the winding number for $n = N$ is either 0 or 1. This is due to the fact that y lies outside the disk $\mathbb{D}(C(a); \epsilon/4)$ where the polygonal closed curve $C_N(a_N, b_N)$ may intersect itself. □

A similar result holds for the winding numbers with respect to $D_n(a_n, b_n)$.

LEMMA 4.3. *Let $y \in \mathbb{R}^2 \backslash (C([0, a]) \cup C([b, 1]))$. Then, the sequence $(W(y, D_n(a_n, b_n)))_{n \geqslant 0}$ is eventually well-defined and constant of value either 0 or 1.*

By the above lemmata, we can define the winding numbers

$$W(y, C([a, b])) := \lim_{n \to \infty} W(y, C_n(a_n, b_n)) \qquad \text{and}$$

$$W(y, C([0, a]) \cup C([b, 1])) := \lim_{n \to \infty} W(y, D_n(a_n, b_n)).$$

The next lemma asserts that the winding numbers defined with respect to the above fractal curves have the same expected properties as winding numbers with respect to polygonal curves.

LEMMA 4.4. *Let L be either the curve $C([a, b])$ or the curve $C([0, a]) \cup C([b, 1])$. Let $x, y \in \mathbb{R}^2$ belong to the same connected component of $\mathbb{R}^2 \backslash L$. Then,*

$$W(x, L) = W(y, L).$$

Proof. In the following, for $n \geqslant 0$, L_n denotes the polygonal curve $C_n(a_n, b_n)$ in the case $L = C([a, b]))$ and the polygonal curve $D_n(a_n, b_n)$ in the case $L = C([0, a]) \cup C([b, 1])$.

By Lemmas 4.2 and 4.3, there exists n_0 such that, for all $n \geqslant n_0$, we have

$$W(x, L_n) = W(x, L) \quad \text{and} \quad W(y, L_n) = W(y, L).$$

Since x and y belong to the same component U of $\mathbb{R}^2 \backslash L$, there exists a simple arc $l : [0, 1] \to U$ satisfying $l(0) = x$ and $l(1) = y$. Let $\epsilon > 0$, such that $\text{dist}_H(l([0, 1]), L) > \epsilon$. Remember that $(L_n)_{n \geqslant 0}$ converges to L in Hausdorff distance. Thus, there exists $n_1 \geqslant n_0$ satisfying

$$\text{dist}_H(l([0, 1]), L_{n_1}) \geqslant \epsilon.$$

Therefore, x and y belong to the same connected component of $\mathbb{R}^2 \backslash L_{n_1}$. As L_{n_1} is a polygonal curve, this implies that $W(x, L_{n_1}) = W(y, L_{n_1})$, and hence that $W(x, L) = W(y, L)$.   □

Since we assume that no pairs of identifications are crossing, the following proposition holds (see Figure 1).

PROPOSITION 4.5. *There exist $w_{a,b}, w'_{a,b} \in \{0, 1\}$ such that for all $t \in [0, a) \cup (b, 1]$ and for all $t' \in (a, b)$,*

$$W(C(t), C([a, b])) = w_{a,b} \qquad and \qquad W(C(t'), C([0, a]) \cup C([b, 1])) = w'_{a,b}.$$

$$w_{a,b} = 0 = w'_{a,b} \qquad\qquad w_{a,b} = 1, w'_{a,b} = 0$$
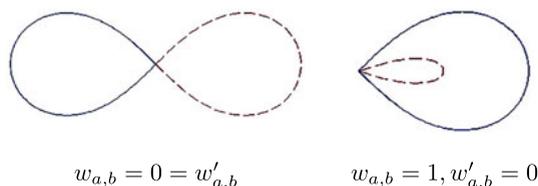
Figure 1.
Proposition 4.5. In the above two cases, $C([a, b])$ is shown solid and
$C([0, a]) \cup C([b, 1])$ is shown dashed. The intersection point is $C(a) = C(b)$.

Proof. We call $K := C([a, b])$ and $J := C([0, a] \cup [b, 1])$ the connected
subcurves of $\partial \mathcal{T}$. By the noncrossing assumption, we have

$$K \cap J = \{C(a) = C(b)\} =: \{x\},$$
$$K \subset (\mathbb{R}^2 \backslash J) \cup \{x\},$$
$$J \subset (\mathbb{R}^2 \backslash K) \cup \{x\}.$$

Note that $K \backslash \{x\} = C((a, b))$; hence, this set is connected. Similarly, $J \backslash \{x\}$
is connected. We call

- U the connected component of $\mathbb{R}^2 \backslash J$ such that $K \backslash \{x\} \subset U$;
- V the connected component of $\mathbb{R}^2 \backslash K$ such that $J \backslash \{x\} \subset V$.

In particular, $K \subset U \cup \{x\}$ and $J \subset V \cup \{x\}$. The proposition now follows
from Lemma 4.4. □

DEFINITION 4.6. Let (a, b) be an identification, and let $w_{a,b}$ be as in
Proposition 4.5. We say that (a, b) is an *outer identification* if $w_{a,b} = w'_{a,b} = 0$.

This case is illustrated on the left side of Figure 1.

THEOREM 2. *Given an identification of C, we can decide whether it is
an outer identification by an algorithm.*

Proof. We show that we can compute $w_{a,b}$ (and similarly $w'_{a,b}$) by an
algorithm. This is proved by a slight modification of the proof of Theorem 1.
Let $y := C(t)$ for some $t \in [0, a) \cup (b, 1]$. Let u_n, v_n be the walks in $G(\mathcal{R}^o)$
satisfying

$$\phi^{(1)}(u_n) = a_n, \qquad \phi^{(1)}(v_n) = b_n.$$

Here, $\phi^{(1)}$ is the Dumont–Thomas number system defined on p. 5. Let k, λ, r
be as in the proof of Theorem 1. Again, we assume, without loss of generality,

that $k = 1$. Then, for all $m \geqslant 1$,

$$C([a,b]) \subset F_m' := \bigcup_{s \in \mathcal{R}} \bigcup_{\substack{w := s \xrightarrow{d_1 | \mathbf{o_1}} s_1 \xrightarrow[u_n \leqslant_{lex} w \leqslant_{lex} v_n]{d_2 | \mathbf{o_2}} \cdots \xrightarrow{d_m | \mathbf{o_m}} s_m \in G(\mathcal{R})^o,}}$$

$$\times \left(\lambda^m \mathbb{D}_r + A^{-1} d_1 + \cdots + A^{-m} d_m \right).$$

The following arguments from the proof of Theorem 1 remain valid:

$$\mathrm{dist}(y, F_m') \geqslant \mathrm{dist}(y, C([a,b])) - 2r\lambda^m,$$

and we call $N \geqslant 1$ the least integer satisfying $y \notin F_N'$. Then, $\mathrm{dist}(y, C_N(a_N, b_N)) > 0$, because $C_N(a_N, b_N) \subset F_N'$. Moreover, for any $n \geqslant N$, the simple polygonal path $C_n(a_n, b_n) \backslash [C(a_n), C(b_n)]$ (as well as the segment $[C(a_n), C(b_n)]$) can be obtained by continuous deformation (homotopy) of $C_N(a_N, b_N) \backslash [C(a_N), C(b_N)]$ (or of the segment $[C(a_N), C(b_N)]$, respectively) inside F_N'. These homotopies fix the vertices of $C_N(a_N, b_N)$.

We conclude that for all $n \geqslant N$,

$$W(y, C_n(a_n, b_n)) = W(y, C_N(a_N, b_N)) = W(y, C([a,b])).$$

The algorithm for the computation of $w_{a,b} = W(y, C([a,b]))$ reads as follows. We can check by computer whether $y \in F_m'$ or not for $m = 1, 2, \ldots$. The least $m \geqslant 1$ such that $y \notin F_m'$ defines N. Then, we compute the winding number $W(y, C_n(a_n, b_n))$ of y with respect to the closed polygonal curve $C_n(a_n, b_n)$. Its value is equal to $w_{a,b}$.   □

§5. Connected components of $\mathcal{T}^\circ$

In this section, we show that the set of outer identifications is in one to one correspondence with the set of connected components of $\mathcal{T}^\circ$.

THEOREM 3. *Suppose that there are no crossing pairs of identifications. Moreover, let (a, b) and (c, d) be two outer identifications with $a < c < d < b$ such that there is no further identification (x, y) with $a < x < y < c$, $d < x < y < b$ or $a < x < c < d < y < b$. Then, $C([a,c]) \cup C([d,b])$ is a simple closed curve, and it is the boundary of a connected component of $\mathcal{T}^\circ$. Therefore, the closure of this component is homeomorphic to a closed disk.*

This theorem is illustrated in Figure 2.
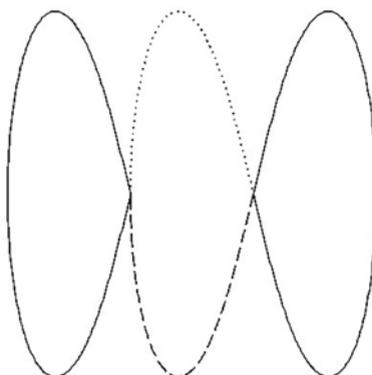
Figure 2.
Theorem 3. $C([a, c])$ is shown dotted and $C([d, b])$ is shown dashed. The
intersection points correspond to $C(a) = C(b)$ and $C(c) = C(d)$.

Proof. By assumption, the parametrization C is injective on each segment $[a, c]$ and $[d, b]$, and the simple closed arcs $C([a, c])$ and $C([d, b])$ meet only at the points $C(a) = C(b)$ and $C(c) = C(d)$. It follows that $C([a, c]) \cup C([d, b])$ is a simple closed curve.

We call this curve L, and call its bounded complementary component B. Then, $L = \partial B$ by Jordan's curve theorem. Let us show in two steps that $B \subset \mathrm{int}(\mathcal{T})$.

(1) We prove that $B \cap \partial \mathcal{T} = \emptyset$. Otherwise, there is t such that

$$x_0 := C(t) \in B \cap \partial \mathcal{T},$$

and, by definition, $t \in [0, a) \cup (c, d) \cup (b, 1]$. First, suppose that $t \in [0, a) \cup (b, 1]$. By our assumptions, we can apply Proposition 4.5 and obtain that

$$W(x_0, C([a, b])) = w_{a,b} = 0 = w_{c,d} = W(x_0, C([c, d])).$$

However, since x_0 is in the bounded component of the simple closed curve L, its winding number with respect to L is $W(x_0, L) = 1$. It follows that

$$0 = W(x_0, C([a, b])) = W(x_0, C([c, d])) + W(x_0, L) = 0 + 1 = 1,$$

a contradiction. Hence, $t \notin [0, a) \cup (b, 1]$. In the same way, using the fact that $w'_{a,b} = w'_{c,d} = 0$, one can prove that $t \notin (c, d)$. Therefore, we conclude that $B \cap \partial \mathcal{T} = \emptyset$.

(2) We prove that $B \cap \text{int}(\mathcal{T}) \neq \emptyset$. Suppose, on the contrary, that $B \cap \text{int}(\mathcal{T}) = \emptyset$. Let $x \in L \backslash \{C(a) = C(b)\}$, and let $\epsilon > 0$, such that

$$\mathbb{D}(x, \epsilon) \cap C([0, a] \cup [b, 1]) = \mathbb{D}(x, \epsilon) \cap C([c, d]) = \emptyset.$$

Since $L \subset \partial \mathcal{T}$, we have that $\text{int}(\mathcal{T}) \cap \mathbb{D}(x, \epsilon) \neq \emptyset$. Let z be in this intersection. Then, by assumption, z is in the unbounded complementary component of the simple closed curve L; hence, $W(z, L) = 0$. Moreover,

$$W(z, C([0, a] \cup [b, 1])) = W(x, C([0, a] \cup [b, 1])) = w'_{a,b} = 0$$

and

$$W(z, C([c, d])) = W(x, C([c, d])) = w_{c,d} = 0.$$

We use here the fact that (a, b) and (c, d) are outer identifications. Therefore,

$$W(z, \partial \mathcal{T}) = W(z, C([0, a] \cup [b, 1])) + W(z, L) + W(z, C([c, d])) = 0.$$

However, since z is an inner point of $\mathcal{T}$, we have $W(z, \partial \mathcal{T}) = 1$, a contradiction. We conclude that $B \cap \text{int}(\mathcal{T}) \neq \emptyset$.

This proves that $B \subset \text{int}(\mathcal{T})$. Consequently, B is a connected component of $\text{int}(\mathcal{T})$, as it is an open connected set of $\text{int}(\mathcal{T})$ whose boundary is a subset of $\partial \mathcal{T}$. The fact that its closure is a topological disk follows from the theorem of Schönflies. ∎

§6. An example from Bandt and Gelbrich

This example can be found in [BG94] and [BW01, Figure 4]. We depict it with its neighbors in Figure 3.

The tile $\mathcal{T}$ satisfies the equation

$$A\mathcal{T} = \bigcup_{a \in \mathcal{D}} (\mathcal{T} + a),$$

where

$$(6.1) \qquad A = \begin{pmatrix} 0 & 3 \\ 1 & 1 \end{pmatrix}, \qquad \mathcal{D} = \left\{ \begin{pmatrix} 0 \\ 0 \end{pmatrix}, \begin{pmatrix} 1 \\ 0 \end{pmatrix}, \begin{pmatrix} -1 \\ 0 \end{pmatrix} \right\}.$$

The tile $\mathcal{T}$ has the following neighbors:

$$(6.2) \quad \mathcal{S} = \left\{ \pm \begin{pmatrix} 1 \\ 0 \end{pmatrix}, \pm \begin{pmatrix} -2 \\ 1 \end{pmatrix}, \pm \begin{pmatrix} -1 \\ 1 \end{pmatrix}, \pm \begin{pmatrix} -4 \\ 2 \end{pmatrix}, \pm \begin{pmatrix} -3 \\ 1 \end{pmatrix} \right\}.$$
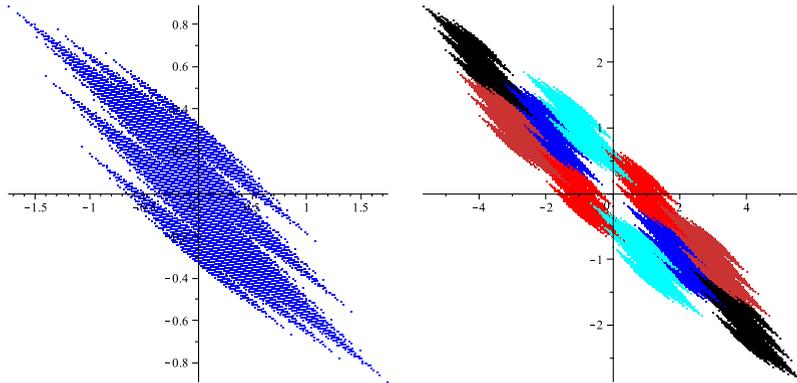
Figure 3.
Example of Bandt and Gelbrich and its lattice tiling.
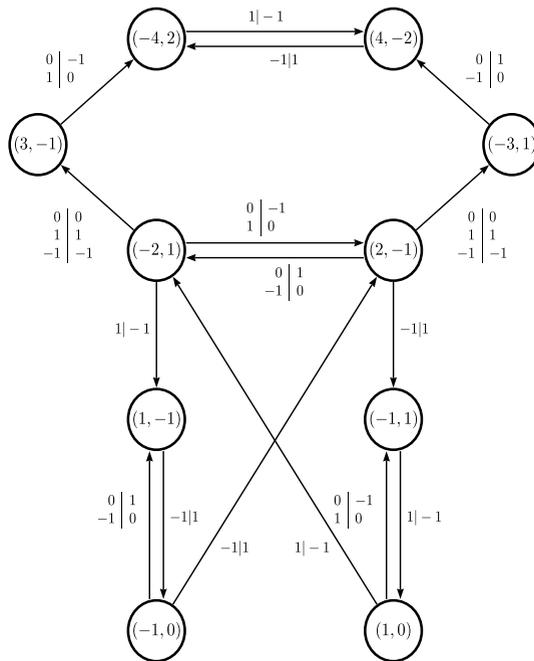
Figure 4.
Boundary graph of the example of Bandt and Gelbrich.

The contact automaton and the boundary automaton can be computed via well-known algorithms (see, for example, [ST03]). The boundary automaton $G(\mathcal{S})$ is depicted in Figure 4. The contact automaton $G(\mathcal{R})$ is the restriction

of the boundary automaton to the set

$$(6.3) \qquad \mathcal{R} = \left\{ \pm \begin{pmatrix} 1 \\ 0 \end{pmatrix}, \pm \begin{pmatrix} -2 \\ 1 \end{pmatrix}, \pm \begin{pmatrix} -1 \\ 1 \end{pmatrix} \right\}.$$

As $G(\mathcal{R})$ is the contact automaton of $\mathcal{T}(A, \mathcal{D})$, $\partial\mathcal{T}$ is the solution of the GIFS (2.1). Since $\det(A) < 0$, the orientation of the boundary pieces changes at each iteration of (2.1). We model this flipping by doubling the number of states of the contact automaton (see also [AL10, Section 2]) as follows.

- For each state $s \in \mathcal{R}$, we create the states s and $\overline{s}$.
- For each transition $s \xrightarrow{a|a'} s' \in G(\mathcal{R})$, we create the transitions $s \xrightarrow{a|a'} \overline{s'}$ and $\overline{s} \xrightarrow{a|a'} s'$.

The resulting automaton then has 12 states. It is also a GIFS for the boundary, but each boundary part K_s is duplicated ($K_s = K_{\overline{s}}$). This automaton can be ordered as in Figure 5 to perform the boundary parametrization. We denote by $R := \{1, 2, \dots, \overline{5}, \overline{6}\}$ the set of states of this ordered extension $G(\mathcal{R})^o$. It follows that $\partial\mathcal{T}$ satisfies

$$\begin{cases} \partial\mathcal{T} = \displaystyle\bigcup_{i=1}^{6} K_i, \\ K_i = \displaystyle\bigcup_{i \xrightarrow{a||\mathbf{o}} j \in G(\mathcal{R})^o} A^{-1}(K_j + a) \quad (i \in R). \end{cases}$$

Note that

$$K'_{s^1} = K_1 = K_{\overline{1}}, \dots, K'_{s^6} = K_6 = K_{\overline{6}}.$$

The following theorem justifies Assumptions 1 and 2.

THEOREM 4. *Let $\mathcal{T} = \mathcal{T}(A, \mathcal{D})$ be the self-affine tile associated to the data (6.1). Let $\beta := \frac{1+\sqrt{13}}{2}$. Then, there exist a $C : [0, 1] \to \partial\mathcal{T}$ Hölder continuous onto mapping with $C(0) = C(1)$ and a hexagon $Q \subset \mathbb{R}^2$ with the following properties. Let $(\mathcal{T}_n)_{n \geqslant 0}$ be the sequence of approximations of $\mathcal{T}$ associated to Q; that is, $\mathcal{T}_0 := Q$ and, for $n \geqslant 1$, $\mathcal{T}_n$ is defined by*

$$A\mathcal{T}_n := \bigcup_{a \in \mathcal{D}} (\mathcal{T}_{n-1} + a).$$

Then, we have the following.
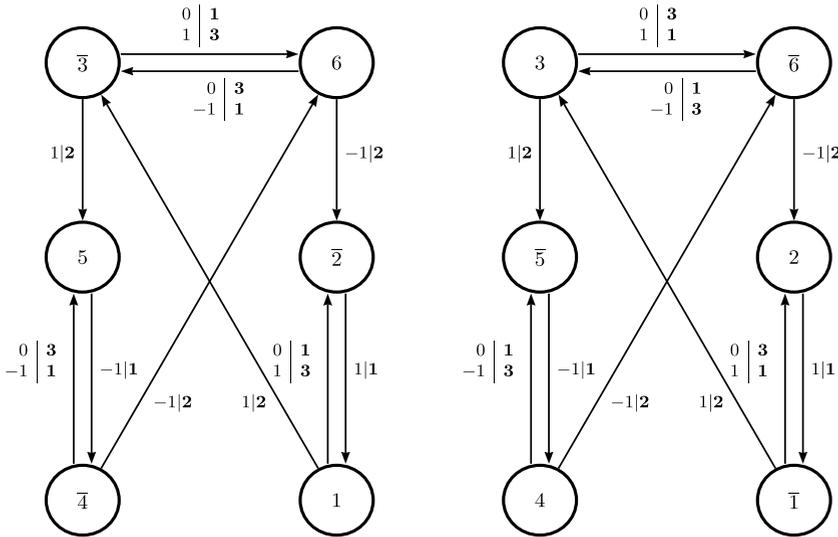
Figure 5.
Ordered extension $G(\mathcal{R})^o$ for the example of Bandt and Gelbrich.

(1) $\lim_{n\to\infty} \mathcal{T}_n = \mathcal{T}$ and $\lim_{n\to\infty} \partial\mathcal{T}_n = \partial\mathcal{T}$ *(in Hausdorff metric).*

(2) *Denote by V_n the set of vertices of $\partial\mathcal{T}_n$. For all $n \in \mathbb{N}$, $V_n \subset V_{n+1} \subset C(\mathbb{Q}(\beta) \cap [0,1])$ (i.e., the vertices have $\mathbb{Q}(\beta)$-addresses in the parametrization).*

(3) *For all $n \geqslant 0$, $\partial\mathcal{T}_n$ is a simple closed curve.*

Proof. $G(\mathcal{R})^o$ is the union of two strongly connected components. Each component has the same irreducible incidence matrix $\mathbf{C}$, whose Perron–Frobenius eigenvalue $\beta = \frac{1+\sqrt{13}}{2}$ is the largest root of the characteristic polynomial $x^6 - 8x^4 + 16x^2 - 9$. Therefore, the incidence matrix $\mathbf{D}$ of $G(\mathcal{R})^o$ has a strictly positive left eigenvector $\mathbf{u} = (u_1, \ldots, u_6, u_{\overline{1}}, \ldots, u_{\overline{6}})$ associated to β, which can be chosen such that $u_1 + \cdots + u_6 = 1$. This is sufficient to perform the parametrization procedure (see [AL10] for more details). We just need to check the compatibility conditions of Definition 2.3 with $p = 12$, together with the additional compatibility condition

$$(6.4) \qquad\qquad \psi(6; \overline{\mathbf{o_m}}) = \psi(1; \overline{\mathbf{1}}).$$

Here, ψ is naturally defined as in Section 2. All of these compatibility conditions consist of showing that pairs of digit sequences $(a_n)_{n\geqslant 1}$ and

$(a'_n)_{n \geqslant 1}$ lead to the same boundary point; that is,

$$\sum_{n \geqslant 1} A^{-n} a_n = \sum_{n \geqslant 1} A^{-n} a'_n.$$

This can be checked on the automata depicted in Figures 7 and 8. We refer to Proposition 6.3 for the construction of these automata. Applying Theorem 2.4, we obtain the existence of the Hölder parametrization $C :$ $[0, 1] \to \partial T$ with $C(0) = C(1)$.

The hexagon Q is defined in Proposition 6.1 and depicted in Figure 10. The first part of Item (1) is then just the consequence that $\mathcal{T}$ is the attractor of the iterated function system (IFS) $\{x \mapsto A^{-1}(x + a)\}_{a \in \mathcal{D}}$.

The second part of Item (1) as well as Item (2) can be proved as in [AL11, Proposition 5.7]. This consists of showing for all $n \geqslant 0$ that $\partial \mathcal{T}_n$ is equal to Δ_n, the sequence of boundary approximations given by Theorem 2.4.

Item (3) can be proved similarly to [AL11, Proposition 5.6]. The proof relies on the fact that the hexagon Q induces a tiling by its translations in which the neighboring tiles have a one-dimensional intersection (see Proposition 6.1 and Figure 10). One then uses the property that $A^n \mathcal{T}_n$ is a connected union of translations of the hexagon Q and has therefore, as well as $\mathcal{T}_n$, a connected interior. □

PROPOSITION 6.1.   *For $i \in \{1, 2, 3, 4, 5, 6\}$, let $C_i := \psi(i; \overline{\mathbf{1}})$, and let $[C_1, \ldots, C_6, C_1]$ be the polygonal curve obtained by joining the points $C_1, \ldots, C_6, C_1$ in this order. Then, $[C_1, \ldots, C_6, C_1]$ is a simple closed curve. Let Q be the closure of its bounded complementary component. Then, Q tiles $\mathbb{R}^2$ by $\mathbb{Z}^2$. Moreover, the neighbors of Q in this tiling are the tiles $Q + s$ with $s \in \mathcal{R}$, and*

$$\partial Q = \bigcup_{s \in \mathcal{R}} Q \cap (Q + s).$$

Proof.   We compute

$$C_1 = (1, -1/3), \qquad C_2 = (0, 1/3), \qquad C_3 = (-1, 2/3),$$
$$C_4 = (-1, 1/3), \qquad C_5 = (0, -1/3), \qquad C_6 = (1, -2/3).$$

Joining the points $C_1, C_2, \ldots, C_6, C_1$ in this order yields a simple closed curve. The closure of the bounded component of its complement in $\mathbb{R}^2$ is a hexagon Q depicted in Figure 10. Consider the quadrilateral H_1 with vertices

C_6, C_1, C_2, C_3 and the quadrilateral H_2 with vertices C_3, C_4, C_5, C_6. Then $H_1 \cup (H_2 + (-1, 1))$ is a parallelogram which obviously tiles the plane by $\mathbb{Z}^2$. It follows that Q itself tiles the plane by $\mathbb{Z}^2$. $\qquad\square$

As mentioned in the proof of Theorem 4, checking the compatibility conditions $\psi(w) = \psi(w')$ in Definition 2.3 amounts to proving equalities of the form $\sum_{n\geqslant 1} A^{-n} a_n = \sum_{n\geqslant 1} A^{-n} a'_n$ for sequences of digits $(a_n), (a'_n)$. Moreover, for topological purposes, we look for all pairs of parameters (t, t') with $t \neq t' \in [0, 1)$ fulfilling $C(t) = C(t')$ (noninjectivity points). This requires us to find all pairs (w, w') of walks $w, w' \in G(\mathcal{R})^o$ satisfying $\psi(w) = \psi(w')$ other than the pairs (w, w') of walks considered in the compatibility conditions. The right context for these computations is the framework of Büchi automata.

DEFINITION 6.2. Let $\mathcal{A} = (S, \Lambda, E)$ be an automaton; that is, S is a finite set of *states*, Λ is a finite set of *labels* and $E \subset S \times \Lambda \times S$ is the set of *transitions*. Note that for $(t, l, t') \in E$, we usually write $t \xrightarrow{l} t'$. Let $I, F \subset S$. Then, (S, Λ, E, I, F) is called a *Büchi automaton* with the set of *initial states* I and the set of *final states* F. An infinite walk

$$V : t_1 \xrightarrow{l_1} t_2 \xrightarrow{l_2} \cdots$$

in the automaton $\mathcal{A}$ is called *admissible* if it starts from a state of I ($t_1 \in I$) and visits F infinitely often. (This means that $\{t_n ; n \geqslant 1\} \cap F$ is infinite.)

A Büchi automaton $\mathcal{I}^\psi$ collects all pairs (w, w') of distinct walks w, w' in $G(\mathcal{S})$ (Figure 4) whose sequences of labels $(a_n), (a'_n)$ fulfill $\sum_{n\geqslant 1} A^{-n} a_n = \sum_{n\geqslant 1} A^{-n} a'_n$ (Figure 6). To infer from this automaton the pairs of parameters (t, t') satisfying $t \neq t'$ and $C(t) = C(t')$, we transfer it to Büchi automata built up from $G(\mathcal{R})^o$. A Büchi automaton $\mathcal{A}^\psi$ collects all pairs (w, w') of distinct walks $w, w' \in G(\mathcal{R})^o$ satisfying $\psi(w) = \psi(w')$ and corresponding to different sequences of digits $(a_n), (a'_n)$ (Figure 7). Another Büchi automaton $\mathcal{A}^{sl}$ collects all pairs (w, w') of distinct walks $w, w' \in G(\mathcal{R})^o$ satisfying $\psi(w) = \psi(w')$ and corresponding to the same sequence of digits $(a_n), (a'_n) = (a_n)$ (Figure 8). Erasing from $\mathcal{A}^\psi \cup \mathcal{A}^{sl}$ the pairs of walks (w, w') corresponding to the compatibility conditions (Definition 2.3), we obtain the desired pairs of walks associated with all pairs of parameters (t, t') with $t \neq t' \in [0, 1)$ and fulfilling $C(t) = C(t')$. This operation of "erasing" is related to the so-called *complementation of Büchi automata*, which can be a difficult task in general. However, it turns out to be easy in our example (see Definition 6.4, Proposition 6.5 and the paragraph between them).
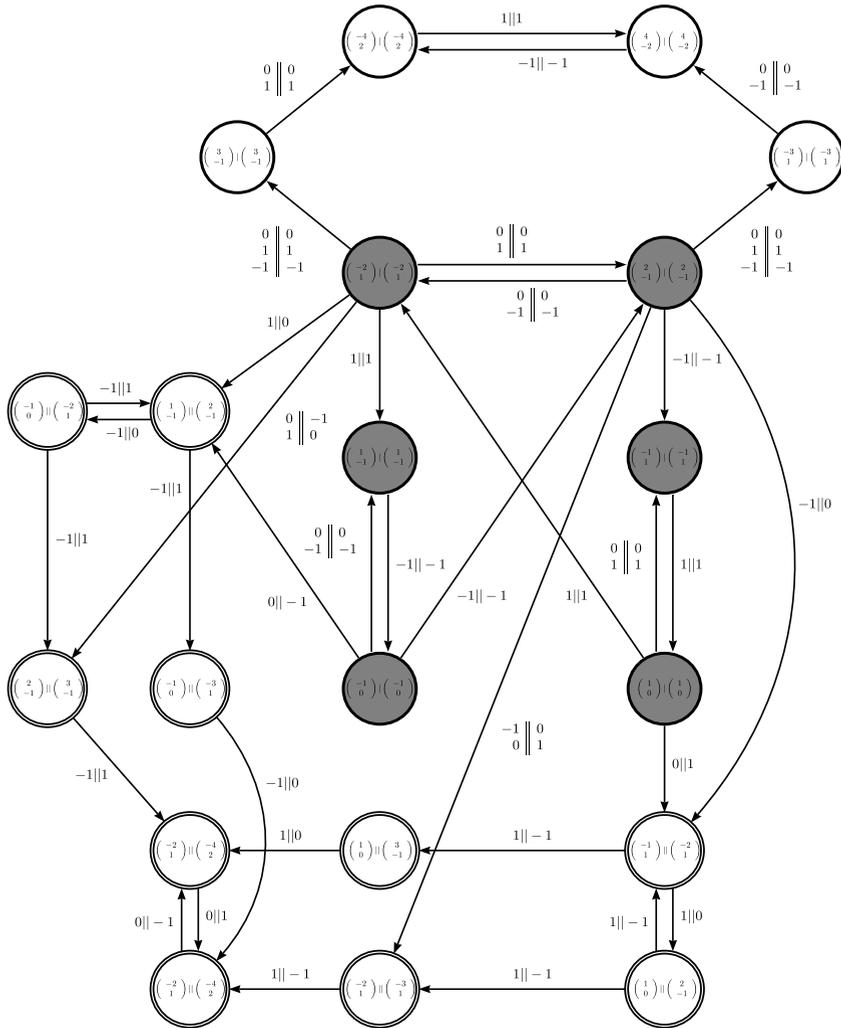
Figure 6.
Example of Bandt and Gelbrich: automaton $\mathcal{I}^{\psi}$.

PROPOSITION 6.3. *Let $w \neq w'$ infinite walks in $G(\mathcal{R})^o$ with*

$$w : i \xrightarrow{a_1 || \mathbf{o_1}} \cdots$$

and

$$w' : j \xrightarrow{a'_1 || \mathbf{o_1}'} \cdots ,$$
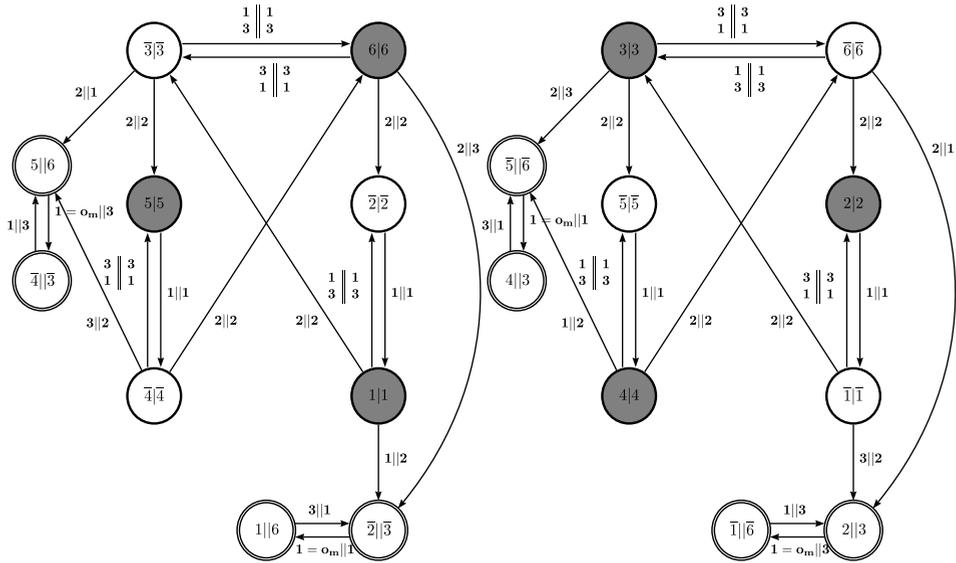
Figure 7.
Example of Bandt and Gelbrich: automaton $\mathcal{A}^{\psi}$.

where $i, j \in \{1, 2, 3, 4, 5, 6\}$. Then, $\psi(w) = \psi(w')$ if and only if, up to permutation of w and w', one of the following holds.

- $i = j$ and

$$(6.5) \qquad i|i \xrightarrow{\mathbf{o_1}||\mathbf{o_1'}} \cdots$$

is an admissible walk in $\mathcal{A}^{\psi}$ depicted in Figure 7.
- The walk

$$(6.6) \qquad i|j \xrightarrow{\mathbf{o_1}||\mathbf{o_1'}} \cdots$$

is an admissible walk in $\mathcal{A}^{sl}$ depicted in Figure 8.

In both automata, the gray states are the initial states and the double lined states are the final states.

Proof. By definition, $\psi(w) = \psi(w') \Longleftrightarrow \sum_{n \geqslant 1} A^{-n} a_n = \sum_{n \geqslant 1} A^{-n} a_n'$. This point must belong to a boundary part K_{s_0} for some $s_0 \in \mathcal{R}$. Suppose that the digit labels $(a_n)_{n \geqslant 1}$ and $(a_n')_{n \geqslant 1}$ are distinct, and let $m \geqslant 0$ be the least integer such that $a_{m+1} \neq a_{m+1}'$. By Proposition 2.1, there must be

Figure 8.

Example of Bandt and Gelbrich: automaton $\mathcal{A}^{sl}$.

$(a_n'')_{n \geqslant 1} \in \mathcal{D}^{\mathbb{N}}$ and walks

$$s_0 \xrightarrow{a_1|a_1''} s_1 \xrightarrow{a_2|a_2''} \cdots \xrightarrow{a_m|a_m''} s_m \xrightarrow{a_{m+1}|a_{m+1}''} s_{m+1} \rightarrow \cdots,$$

$$s_0 \xrightarrow{a_1'=a_1|a_1''} s_1 \xrightarrow{a_2'=a_2|a_2''} \cdots \xrightarrow{a_m'=a_m|a_m''} s_m \xrightarrow{a_{m+1}'|a_{m+1}''} s_{m+1}' \rightarrow \cdots$$

in $G(\mathcal{S})$. As proved in [AL11, Section 4], these pairs of walks are recognized as the admissible walks of a Büchi automaton $\mathcal{I}^\psi$, depicted in Figure 6.

Note that some pairs of walks (w, w') recognized by $\mathcal{I}^\psi$ satisfy $w' \in \mathcal{G}(\mathcal{S}) \backslash \mathcal{G}(\mathcal{R})$. However, it is easy to check that the corresponding digit sequence $(a'_n)_{n \geqslant 1}$ of such a w' does not appear as a digit sequence of any other walk of $G(\mathcal{S})$. We therefore delete these pairs of walks from $\mathcal{I}^\psi$ and obtain the automaton $\mathcal{A}^\psi$ of Figure 7. In this figure, we use for the states and edges the elements of the ordered extension $G(\mathcal{R})^o$. Pairs of infinite walks (w, w'), $w \neq w'$ in $G(\mathcal{R})^o$ both starting in $\{1, 2, 3, 4, 5, 6\}$, having distinct digit sequences $(a_n)_{n \geqslant 1} \neq (a'_n)_{n \geqslant 1}$ and satisfying $\psi(w) = \psi(w')$, are of the form (6.5).

For $w \neq w'$ infinite walks in $G(\mathcal{R})^o$ with $\psi(w) = \psi(w')$ and identical digit sequences $(a_n)_{n \geqslant 1} = (a'_n)_{n \geqslant 1}$, we construct the automaton $\mathcal{A}^{sl}$ as in [AL11] and depict it in Figure 8. □

The pairs (w, w') of walks $w, w' \in G(\mathcal{R})^o$ associated to the compatibility conditions (Definition 2.3) are called trivial identifications, according to the following definition.

DEFINITION 6.4. Let $w \neq w'$ be two walks of $G(\mathcal{R})^o$ starting in $\{1, 2, 3, 4, 5, 6\}$ and satisfying the equality $\psi(w) = \psi(w')$. We call the pair (w, w') *trivial identification (in the Dumont–Thomas number system)* if, up to permutation of w and w', there is a walk w_0 of length n in $G(\mathcal{R})^o$ such that

$$w = w_0 \& \overline{\mathbf{o_m}}, \qquad w' = w_0^+ \& \overline{\mathbf{1}}.$$

Here, w_0^+ is the next walk of length n in lexicographical order in $G(\mathcal{R})^o$. By convention,

$$(6; \underbrace{\mathbf{o_m}, \ldots, \mathbf{o_m}}_{n \text{ times}})^+ := (1; \underbrace{\mathbf{1}, \ldots, \mathbf{1}}_{n \text{ times}}).$$

By definition, the walks of a trivial identification are associated to the same parameter $t \in [0, 1]$ in our parametrization. On the contrary, nontrivial identifications make the parametrization noninjective. Finding out the nontrivial identifications can be a difficult task: it is related to the complementation of Büchi automata. In our example, it is easy to see that $\mathcal{A}^\psi$ only gives rise to trivial identifications. Moreover, the identifications in $\mathcal{A}^{sl}$ depicted in the top part of Figure 8 only give rise to trivial identifications. However, in the bottom part, we can find the following nontrivial identifications.

PROPOSITION 6.5. *The pair (w, w') is a nontrivial identification in the Dumont–Thomas number system if and only if it is a pair of Figure 9, up to*

	w	w'	
$n \geq 0$	$P_n = (1; (\mathbf{3,1})^n, \mathbf{2,3}, \overline{(\mathbf{3,1})})$	$P'_n = (2; (\mathbf{1,1})^n, \mathbf{1,2}, \overline{(\mathbf{3,1})})$	$\xrightarrow{n\to\infty}$ $(1; \underbrace{\overline{(\mathbf{3,1})}}_{\overline{\mathbf{o_m}}}) = (2; \overline{\mathbf{1}}) \cong (0, 1/3) \in \mathcal{T}$
$n \geq 0$	$Q_n = (1; (\mathbf{3,1})^n, \mathbf{3,1,2}, \overline{(\mathbf{1,3})})$	$Q'_n = (2; (\mathbf{1,1})^n, \mathbf{1,2,1}, \overline{(\mathbf{1,3})})$	$\xrightarrow{n\to\infty}$ $(1; \underbrace{\overline{(\mathbf{3,1})}}_{\overline{\mathbf{o_m}}}) = (2; \overline{\mathbf{1}})$
	$R = (1; \mathbf{2}, \overline{(\mathbf{1,3})})$	$R' = (3; \mathbf{1}, \overline{(\mathbf{1,3})})$	$\cong (-1/3, 1/3) \in \mathcal{T}$
	$S = (6; \overline{(\mathbf{3,1})})$	$S' = (3; \overline{(\mathbf{3,1})})$	$\cong (0, 0) \in \mathcal{T}$
$n \geq 0$	$T_n = (5; (\mathbf{1,1})^n, \mathbf{1,2}, \overline{(\mathbf{3,1})})$	$T'_n = (4; (\mathbf{3,1})^n, \mathbf{2,3}, \overline{(\mathbf{3,1})})$	$\xrightarrow{n\to\infty}$ $(5; \overline{\mathbf{1}}) = (4; \underbrace{\overline{(\mathbf{3,1})}}_{\overline{\mathbf{o_m}}}) \cong (0, -1/3) \in \mathcal{T}$
$n \geq 0$	$U_n = (5; (\mathbf{1,1})^n, \mathbf{1,2,1}, \overline{(\mathbf{1,3})})$	$U'_n = (4; (\mathbf{3,1})^n, \mathbf{3,1,2}, \overline{(\mathbf{1,3})})$	$\xrightarrow{n\to\infty}$ $(5; \overline{\mathbf{1}}) = (4; \underbrace{\overline{(\mathbf{3,1})}}_{\overline{\mathbf{o_m}}})$
	$V = (6; \mathbf{1}, \overline{(\mathbf{1,3})})$	$V' = (4; \mathbf{2}, \overline{(\mathbf{1,3})})$	$\cong (1/3, -1/3) \in \mathcal{T}$

Figure 9.

Nontrivial identifications in the example of Bandt and Gelbrich.

permutation of w and w'. The associated points in $[0, 1]$ are schematically represented in Figure 9 too. Here, for $i \in \{1, \ldots, 6\}$, the circled number ⓘ stands for the parameter of $[0, 1]$ associated with the walk $(i; \overline{\mathbf{1}})$. No two pairs of identifications are crossing.

Proof. As mentioned above, $\mathcal{A}^{\psi}$ and the part of $\mathcal{A}^{sl}$ at the top of Figure 8 only give rise to trivial identifications. In the bottom part, we find the trivial identifications

$$\psi(1; \overline{\mathbf{o_m}}) = \psi(2; \overline{\mathbf{1}}) \qquad \text{and} \qquad \psi(5; \overline{\mathbf{1}}) = \psi(4; \overline{\mathbf{o_m}}).$$

The other identifications are nontrivial and are listed in Figure 9. □

This allows us to determine all of the *cut points* of $\mathcal{T}$. These are the points $z \in \mathcal{T}$ such that $\mathcal{T} \backslash \{z\}$ is no more connected.

THEOREM 5. *Let $\mathcal{T} = \mathcal{T}(A, \mathcal{D})$ be the tile associated to the data (6.1). For $i \in \{0, 1, -1\}$, we denote by $f_i(x) = A^{-1}(x + (i, 0)^T)$ the corresponding contraction. Then, the sequence of cut points of $\mathcal{T}$ reads as follows ($n \geqslant 0$):*
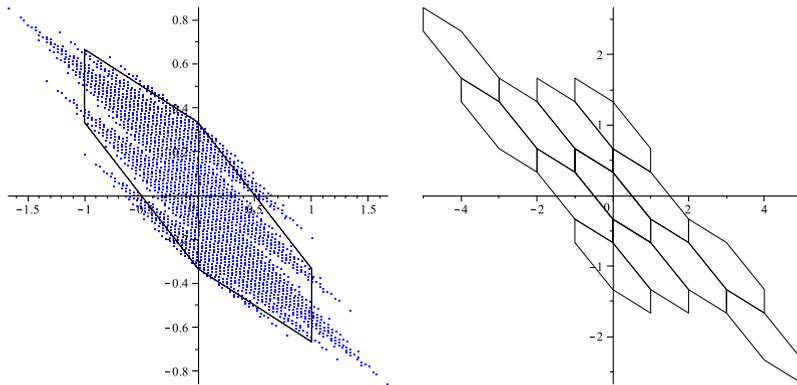
Figure 10.
Example of Bandt and Gelbrich: hexagon Q and associated tiling.

(i) $f_1^{2n+2}((0,0)^T)$;
(ii) $f_1^{2n+3}((0,0)^T)$;
(iii) $f_1((0,0)^T)$;
(iv) $(0,0)^T$;
(v) $f_{-1}^{2n+2}((0,0)^T)$;
(vi) $f_{-1}^{2n+3}((0,0)^T)$;
(vii) $f_{-1}((0,0)^T)$.

Proof. We show that each cut point corresponds to a nontrivial identification listed in Figure 9.

First, note that for every $t \in [0,1]$, $C([0,1]\backslash\{t\})$ remains connected. (Remember that $C(0) = C(1)$.)

Then, consider, for example, the identification (R, R') and the associated values $0 < t_R < t_{R'} < 1$. Denote $z := C(t_R) = C(t_{R'})$. Then, $C([0,1]\backslash\{t_R, t_{R'}\}) = \partial T\backslash\{z\}$ is no more connected: it consists of exactly two connected components, namely $C([0, t_R] \cup (t_{R'}, 1])$ and $C((t_R, t_{R'}))$.

The corresponding sequence of digits is read off from Figure 5: $P(1; \mathbf{2}, \overline{(\mathbf{1}, \mathbf{3})})$ is labeled by the sequence of digits $1\overline{00}$, which is the point $f_1(\mathrm{Fix}(f_0)) = (-1/3, 1/3)$, as $\mathrm{Fix}(f_0) = (0,0)^T$. This corresponds to Item (iii) of the theorem.

This proof holds for every pair of identified walks of Figure 9. Item (i) corresponds to (P_n, P'_n), Item (ii) corresponds to (Q_n, Q'_n), and so on.   □

Furthermore, we can infer the following topological description of the boundary of $\mathcal{T}$.

THEOREM 6.   *The boundary $\partial\mathcal{T}$ of the tile $\mathcal{T} = \mathcal{T}(A, \mathcal{D})$ associated to the data (6.1) is a countable union of simple closed curves, together with two points. These are*

- *the curves $C([a, c] \cup [d, b])$, where $((a, b), (c, d))$ is any pair of* consecutive *nontrivial identifications; that is, $0 < a < c < d < b < 1$ and there is no identification (e, f) satisfying $a < e < c$ and $d < f < b$ (see Figure 9);*
- *the curve $C([t_S, 1] \cup [0, t_R] \cup [t_{R'}, t_{S'}])$, where $t_S, t_R, t_{R'}, t_{S'}$ are associated to the walks S, R, R', S' of Figure 9;*
- *the points $\pm(0, 1/3)$.*

Each curve intersects exactly two other curves, each at one point.

Proof.   This result can be read off from Figure 9. If $((a, b), (c, d))$ is any pair of consecutive nontrivial identifications satisfying $0 < a < c < d < b < 1$, then C is injective on $[a, c]$ and on $[d, b]$. Thus, $C([a, c])$ and $C([d, b])$ are two simple arcs meeting only at their extremities $C(a) = C(b)$ and $C(c) = C(d)$. Their union is therefore a simple closed curve. It meets exactly two other curves, one at $C(a) = C(b)$ and the other one at $C(c) = C(d)$.

Similarly, C is injective on $[t_S, 1] \cup [0, t_R]$ (apart from the trivial identification $C(0) = C(1)$) and on $[t_{R'}, t_{S'}]$. Thus, $C([t_S, 1] \cup [0, t_R])$ and $C([t_{R'}, t_{S'}])$ are two simple arcs meeting only at their extremities $C(t_S) = C(t_{S'})$ and $C(t_R) = C(t_{R'})$. Their union is therefore a simple closed curve. It also meets exactly two other curves.

The point $(0, 1/3)$ corresponds to the infinite walk $(2; \overline{\mathbf{1}})$ and the point $(0, -1/3)$ corresponds to the infinite walk $(5; \overline{\mathbf{1}})$. These are the two accumulation points of the sequence of simple closed curves.

The union of all these curves together with the two points is equal to $C([0, 1]) = \partial\mathcal{T}$; hence, the description is complete.   □

We now pick up one of these simple closed curves and show that it is the boundary of an interior component.

THEOREM 7.   *Let $0 < t_{S'} < t_{V'} < t_V < t_S < 1$ be associated to the infinite walks S', V', V, S of Figure 9. Then, $C([t_{S'}, t_{V'}] \cup [t_V, t_S])$ is the boundary of an interior component of the tile $\mathcal{T} = \mathcal{T}(A, \mathcal{D})$ defined by (6.1). The closure of this component is homeomorphic to a closed disk.*

Proof.   We apply Theorem 3. We just need to prove that (S', S) and (V', V) are outer identifications. This is done by checking that

$$w_{t_{S'}, t_S} = w'_{t_{S'}, t_S} = 1 \qquad \text{and} \qquad w_{t_{V'}, t_V} = w'_{t_{V'}, t_V} = 1.$$
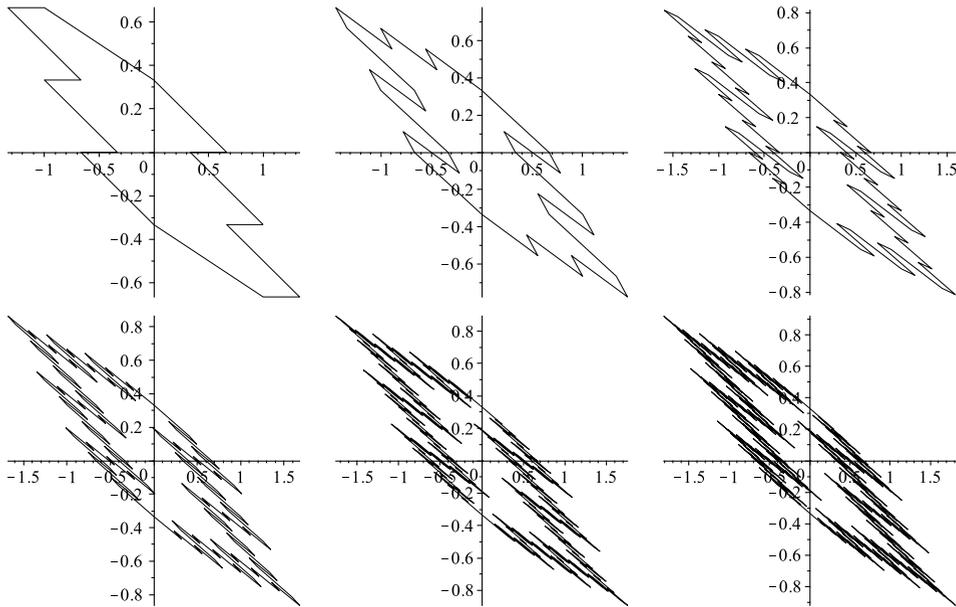
Figure 11.
Example of Bandt and Gelbrich: boundary approximations.

The computations follow the algorithm of Theorem 2. For the identification (S', S), we illustrate them in Figures 12–16. By Proposition 4.5, we can choose rather arbitrarily the reference points on the boundary in order to compute the winding numbers. Let us choose vertices of the hexagon Q as follows:

- $t := t_{C_2}$ $(C_2 = (0, 1/3))$ to compute $w_{t_{S'}, t_S} = W(C(t), C([t_{S'}, t_S]))$;
- $t' := t_{C_5}$ $(C_5 = (0, -1/3))$ to compute $w'_{t_{S'}, t_S} = W(C(t'), C([0, t_{S'}] \cup [t_S, 1]))$.

Figures 12 and 13 show the curves $C_n(a_n, b_n)$ and $D_n(a_n, b_n)$ that are used to compute these winding numbers. To determine which minimal value of n gives us the right winding numbers, we apply the encircling method as described in the proof of Theorem 2. Here, if $|| \cdot ||$ denotes the Euclidean norm, we have

$$||A^{-2}(x, y)|| \leqslant \tfrac{2}{3} ||(x, y)||;$$

hence, $k = 2$ and $\lambda = 2/3$ are suitable. We refer to the proof of Theorem 1 for the definition of these quantities. This allows us to determine a value of r for which $\mathcal{T} \subset \mathbb{D}(0; r)$. Indeed, again with the notations the proof of
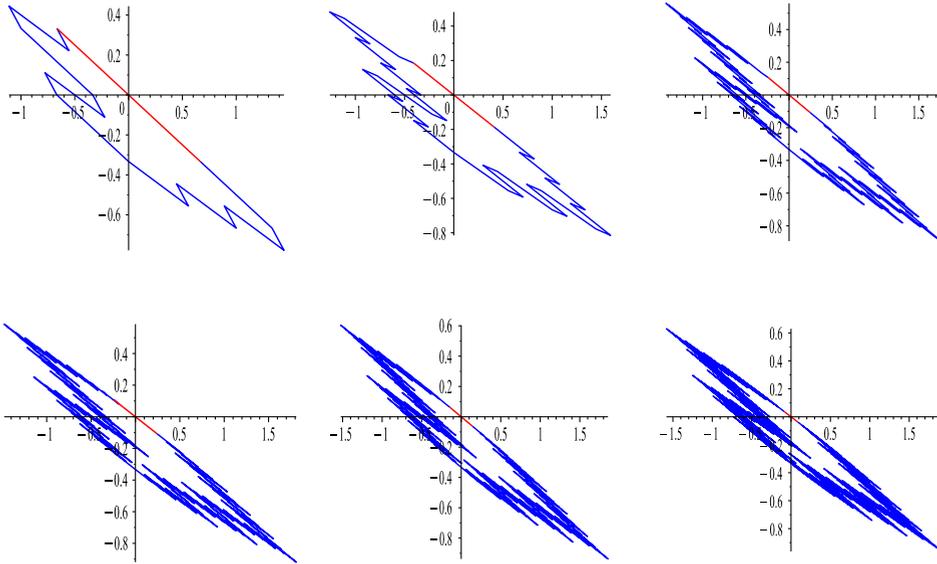
Figure 12.
Example of Bandt and Gelbrich: approximation $C_n(a_n, b_n)$ $(n = 2, 3, 5, 6, 7, 9)$
for $(a, b) = (t_{S'}, t_S)$.

Theorem 1, $A' = A^2, \mathcal{D}' = A\mathcal{D} + \mathcal{D}$, and a point in $\mathcal{T}$ has the norm

$$\left\| \sum_{j \geqslant 1} (A')^{-j} d_j \right\| \leqslant \max_{d, d' \in \mathcal{D}} \{\|Ad + d'\|\} \cdot \sum_{j \geqslant 1} \left(\frac{2}{3}\right)^j = 2\sqrt{2}.$$

Performing the encircling method, we see that for $n = 7$ the reference points lie outside of the covering by the disks (Figures 15 and 16). Computing the winding numbers of the reference points with respect to the approximations $C_7(a_7, a_7)$ and $D_7(a_7, b_7)$, we obtain the value 1 in both cases. Therefore, (S, S') is an outer identification.

Similar computations lead to $w_{t_{V'}, t_V} = w'_{t_{V'}, t_V} = 1$; that is, (V', V) is also an outer identification and Theorem 3 applies. □

REMARK 6.6. In fact, each simple closed curve of Theorem 6 is the boundary of an inner component. In other words, the tile $\mathcal{T}(A, \mathcal{D})$ is a countable union of topological closed disks, together with two points, and each disk intersects exactly two other disks, each at one point. Proving that all of the nontrivial identifications are outer makes use of the self-similarity of $\mathcal{T}$ and involves further computations on the parametrization. Therefore, we postpone the proof to a forthcoming paper.
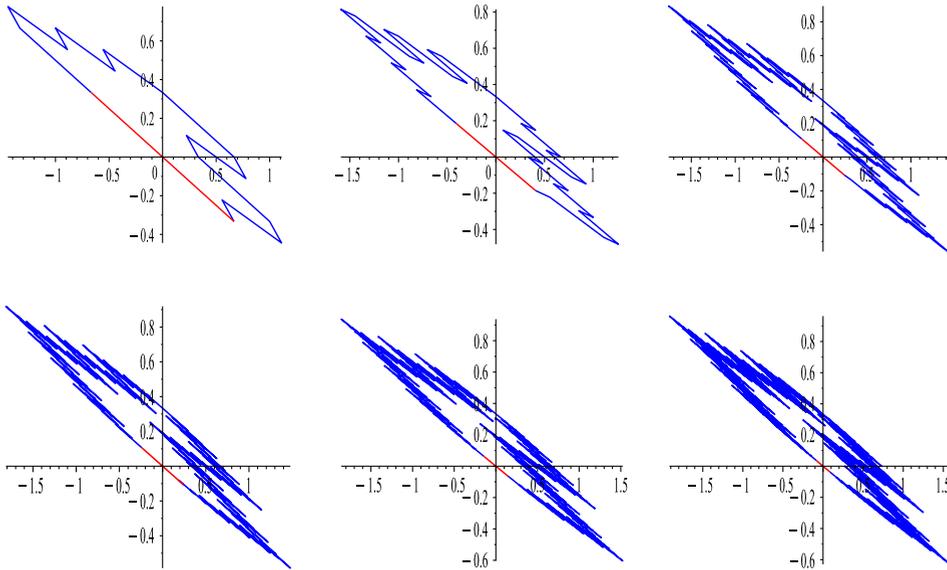
Figure 13.
Example of Bandt and Gelbrich: approximation $D_n(a_n, b_n)$ ($n = 2, 3, 5, 6, 7, 9$)
for $(a, b) = (t_{S'}, t_S)$.

REMARK 6.7.   Theorems 5–7 obtained by our general method can be compared with the work of Ngai and Nguyen [NN03], where the cut points of the Heighway dragon are computed and its interior components are shown to be disklike. To obtain this topological information, Ngai and Nguyen analyze precisely the behavior of n-fold iterations $\mathcal{P}_n$ of the vertical unit segment $\mathcal{P}_0$, whose limit in Hausdorff distance results in the Heighway dragon, and they describe the largest interior component of the Heighway dragon as the attractor of a GIFS. Our method also applies to this example (see Section 7.2), but we rather extract all the information directly from boundary approximations of the Heighway dragon, using our parametrization.

§7. Further work

We give in this section several comments on the paper and present some ideas that will be worked out in forthcoming papers.

7.1 Description of interior components
We aim at developing methods in order to get very precise information on the wild topology of self-affine tiles, like the description of the boundary
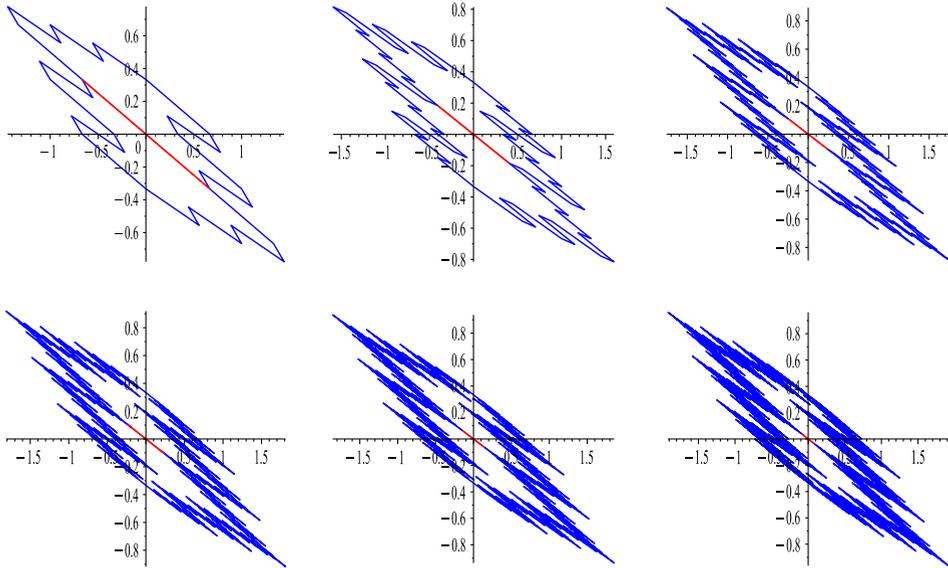
Figure 14.
Example of Bandt and Gelbrich: approximation $C_n(a_n, b_n) \cup D_n(a_n, b_n)$
$(n = 2, 3, 5, 6, 7, 9)$ for $(a, b) = (t_{S'}, t_S)$.

of interior components in terms of GIFSs (see [MW88]). Descriptions of this kind were obtained for the single examples of Figure 18 in [LT08, BLT10] (canonical number system tile of $-2 + i$) or in [NN03] (Heighway dragon). We rather use our general boundary parametrization tool.

7.2 Dealing with nontrivial identifications

In this paper, we restrict to the case where no pairs of identifications are crossing. This first step in the study of non-disklike tiles enables us to describe tiles with a reasonable topological complexity. Similar examples are the *crystallographic replication tiles* (see [Gel94]) depicted in Figure 17. On the left is the Heighway dragon and on the right is a tile found in [LL09, Figure 14]. They tile the plane with respect to the crystallographic groups $p4$ and $p2$, respectively. A boundary approximation of the Heighway dragon obtained via the parametrization method can also be found in this figure.

However, we find in the literature examples where pairs of identifications are crossing. In Figure 18, we depict two such tiles with a wilder topology. The tile at the top is a *canonical number system tile*, associated with the basis $-2 + i$ (see [Gil81]). The intersection of the central tile with some of
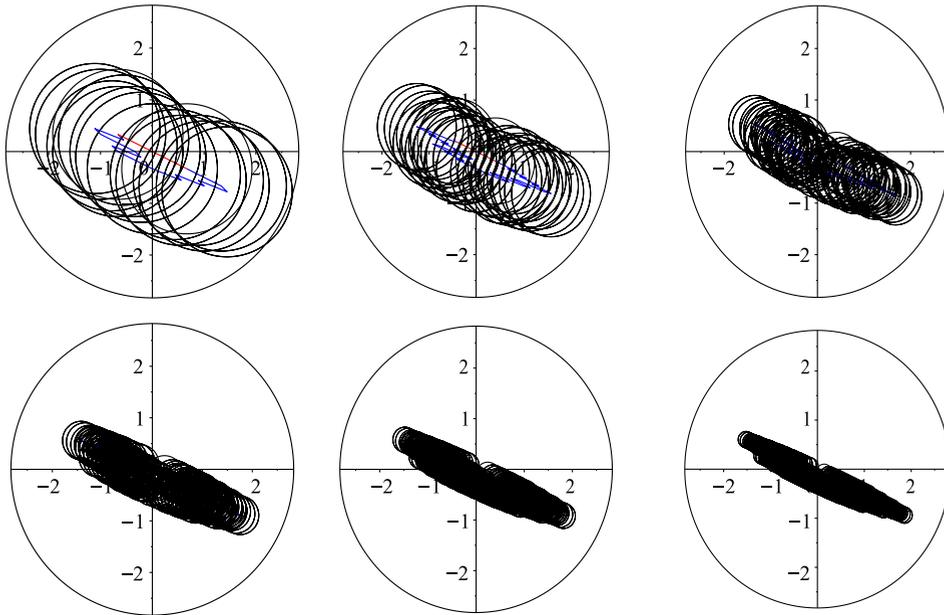
Figure 15.
Example of Bandt and Gelbrich: encircling $C_n(a_n, b_n)$ $(n = 2, 3, 4, 5, 6, 7)$ for
$(a, b) = (t_{S'}, t_S)$.

its neighbors is a Cantor set (see [DLT09]). It has a large set of nontrivial identifications.

At the bottom, we represent an example with an intermediate topological complexity. This self-similar tile Limhex was originally given as a triomino (a polygon composed of regular triangles) tiling generated by a *pseudo* substitution by Socolar (see [Soc]). The substitution rule is depicted in the middle of Figure 18. The substitution is not edge to edge, like the substitution rule of Penrose tiling. Taking the nth iterate and shrinking by the ratio $1/2^n$ to renormalize, we obtain as a Hausdorff limit a fractal tile Limhex, whose IFS is given by

$$f_1(z) = \frac{z}{2}, \qquad f_2(z) = \frac{z-1}{2},$$
$$f_3(z) = \frac{z/w + w^2}{2}, \qquad f_4(z) = -\frac{z/w + w^2}{2},$$

where $w = e^{i\pi/3}$. In Figure 18, we can see the attractor Limhex of this IFS (up to some translation) together with its neighbors in the aperiodic tiling it
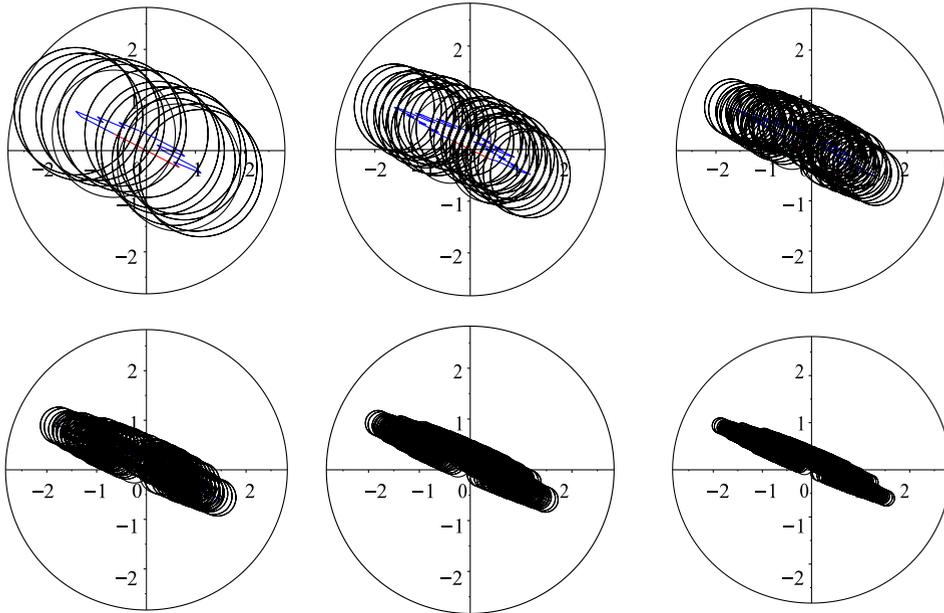
Figure 16.

Example of Bandt and Gelbrich: encircling $D_n(a_n, b_n)$ ($n = 2, 3, 4, 5, 6, 7$) for
$(a, b) = (t_{S'}, t_S)$.
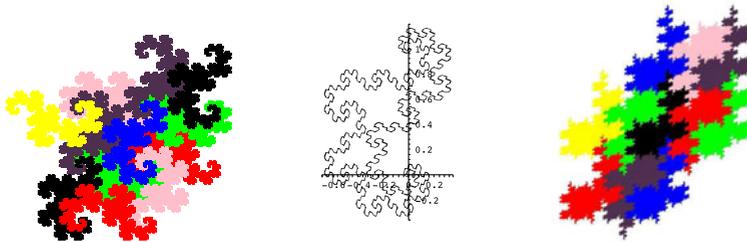
Figure 17.

Tiles with no crossing pairs of identifications.

generates. Here, the intersection of the central tile with a neighbor is either
a simple arc or a single point.

The coming step in our study will be to appropriately extend the
definition of outer identification to such cases. Note that some identifications
on the boundary of the tiles in Figure 18 do not contribute to a new
interior component, but rather lead to a hole. We may call them *inner*
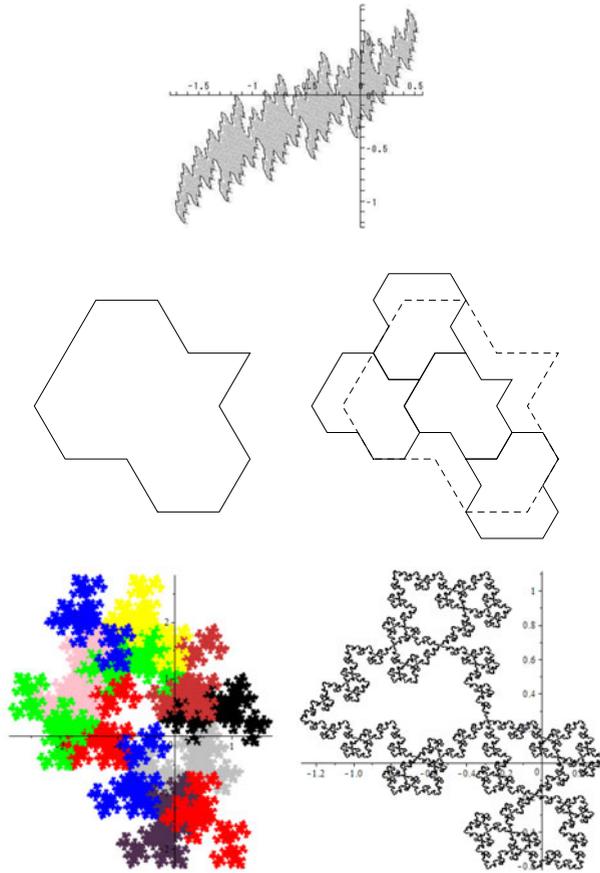
Figure 18.
Tiles with crossing pairs of identifications.

identifications, but, for now, we are looking for typical examples in order to axiomatize and propose the next tractable class of such identifications.

REFERENCES

[Adl98] R. L. Adler, *Symbolic dynamics and Markov partitions*, Bull. Amer. Math. Soc. (N.S.) **35**(1) (1998), 1–56; MR 1477538 (98j:58081).

[AI01] P. Arnoux and S. Ito, *Pisot substitutions and Rauzy fractals*, Bull. Belg. Math. Soc. Simon Stevin **8**(2) (2001), 181–207; Journées Montoises d'Informatique Théorique (Marne-la-Vallée, 2000); MR 1838930 (2002j:37018).

[AL10] S. Akiyama and B. Loridant, *Boundary parametrization of planar self-affine tiles with collinear digit set*, Sci. China Math. **53**(9) (2010), 2173–2194; MR 27 18819.

[AL11]   S. Akiyama and B. Loridant, *Boundary parametrization of self-affine tiles*, J. Math. Soc. Japan **63**(2) (2011), 525–579; MR 2793110 (2012g:37034).

[Ale98]   P. S. Alexandrov, *Combinatorial topology. Vol. 1, 2 and 3*, Dover Publications, Mineola, NY, 1998, translated from the Russian, reprint of the 1956, 1957 and 1960 translations; MR 1643155 (99g:55001).

[Als10]   E. Alster, *The finite number of interior component shapes of the Levy dragon*, Discrete Comput. Geom. **43**(4) (2010), 855–875; MR 2610474 (2011h:28009).

[AS98]   S. Akiyama and T. Sadahiro, *A self-similar tiling generated by the minimal Pisot number*, Acta Math. Info. Univ. Ostraviensis **6** (1998), 9–26.

[AW70]   R. L. Adler and B. Weiss, *Similarity of Automorphisms of the Torus*, Memoirs of the American Mathematical Society **98**, American Mathematical Society, Providence, 1970, MR 0257315 (41 #1966).

[BG94]   C. Bandt and G. Gelbrich, *Classification of self-affine lattice tilings*, J. Lond. Math. Soc. (2) **50**(3) (1994), 581–593; MR 1299459 (95g:52035).

[BKS02]   S. Bailey, T. Kim and R. S. Strichartz, *Inside the Lévy dragon*, Amer. Math. Monthly **109**(8) (2002), 689–703; MR 1927621 (2003f:28011).

[BLT10]   J. Bernat, B. Loridant and J. Thuswaldner, *Interior components of a tile associated to a quadratic canonical number system – Part II*, Fractals **18**(3) (2010), 385–397; MR 2683938.

[BM04]   M. Baake and R. V. Moody, *Weighted Dirac combs with pure point diffraction*, J. Reine Angew. Math. **573** (2004), 61–94; MR 2084582 (2006i:43009).

[Bow70]   R. Bowen, *Markov partitions for Axiom A diffeomorphisms*, Amer. J. Math. **92** (1970), 725–747; MR 0277003 (43 #2740).

[Bow78]   R. Bowen, *Markov partitions are not smooth*, Proc. Amer. Math. Soc. **71**(1) (1978), 130–132; MR 0474415 (57 #14055).

[BW01]   C. Bandt and Y. Wang, *Disk-like self-affine tiles in* $\mathbb{R}^2$, Discrete Comput. Geom. **26**(4) (2001), 591–601; MR 1863811 (2002h:52028).

[Cur06]   E. Curry, *Radix representations, self-affine tiles, and multivariable wavelets*, Proc. Amer. Math. Soc. **134**(8) (2006), 2411–2418; (electronic). MR 2213715 (2007m:52026).

[Dek82a] M. Dekking, *Recurrent sets*, Adv. in Math. **44**(1) (1982), 78–104; MR 654549 (84e:52023).

[Dek82b] M. Dekking, *Replicating superfigures and endomorphisms of free groups*, J. Combin. Theory Ser. A **32**(3) (1982), 315–320; MR 657046 (84i:51019).

[DKV00]   P. Duvall, J. Keesling and A. Vince, *The Hausdorff dimension of the boundary of a self-similar tile*, J. London Math. Soc. (2) **61**(3) (2000), 748–760; MR 176 6102 (2001f:52045).

[DLT09]   S.-J. Duan, D. Liu and T.-M. Tang, *A planar integral self-affine tile with Cantor set intersections with its neighbors*, Integers **9**(A21) (2009), 227–237; MR 2534 911 (2010h:52035).

[DT89]   J.-M. Dumont and A. Thomas, *Systemes de numeration et fonctions fractales relatifs aux substitutions*, Theoret. Comput. Sci. **65**(2) (1989), 153–169; MR 1 020484 (90m:11022).

[Dub93]   S. Dube, *Undecidable problems in fractal geometry*, Complex Systems **7**(6) (1993), 423–444; MR 1307741 (96b:68042).

[Gel94]   G. Gelbrich, *Crystallographic reptiles*, Geom. Dedicata **51**(3) (1994), 235–256; MR 1293800 (95e:52041).

[GH94]   K. Gröchenig and A. Haas, *Self-similar lattice tilings*, J. Fourier Anal. Appl. **1**(2) (1994), 131–170; MR 1348740 (96j:52037).

[Gil81] W. J. Gilbert, *Radix representations of quadratic fields*, J. Math. Anal. Appl. **83**(1) (1981), 264–274; MR 632342 (83m:12005).

[GM92] K. Gröchenig and W. R. Madych, *Multiresolution analysis, Haar bases, and self-similar tilings of* $\mathbf{R}^n$, IEEE Trans. Inform. Theory **38**(2, part 2) (1992), 556–568; MR 1162214 (93i:42001).

[Hut81] J. E. Hutchinson, *Fractals and self-similarity*, Indiana Univ. Math. J. **30**(5) (1981), 713–747; MR 625600 (82h:49026).

[Ken92] R. Kenyon, "*Self-replicating tilings*", in *Symbolic dynamics and its applications (New Haven, CT, 1991)*, Contemp. Math. **135**, American Mathematical Society, Providence, RI, 1992, 239–263. MR 1185093 (94a:52043).

[Ken96] R. Kenyon, *The construction of self-similar tilings*, Geom. Funct. Anal. **6**(3) (1996), 471–488; MR 1392326 (97j:52025).

[KLS15] J. Kellendonk, D. Lenz and J. Savinien, Mathematics of Aperiodic Order, Progress in Mathematics **309**, Birkhäuser, Basel, 2015.

[LL09] B. Loridant and J. Luo, *On a theorem of Bandt and Wang and its extension to p2-tiles*, Discrete Comput. Geom. **41**(4) (2009), 616–642; MR 2496320 (2010d:52044).

[Lor16] B. Loridant, *Topological properties of a class of cubic Rauzy fractals*, Osaka J. Math. **53**(1) (2016), 161–219; MR 3466830.

[LT08] B. Loridant and J. M. Thuswaldner, *Interior components of a tile associated to a quadratic canonical number system*, Topology Appl. **155**(7) (2008), 667–695.

[LW96a] J. C. Lagarias and Y. Wang, *Integral self-affine tiles in* $\mathbb{R}^n$. *I. Standard and nonstandard digit sets*, J. Lond. Math. Soc. (2) **54**(1) (1996), 161–179; MR 1395075 (97f:52031).

[LW96b] J. C. Lagarias and Y. Wang, *Self-affine tiles in* $\mathbf{R}^n$, Adv. Math. **121**(1) (1996), 21–49; MR 1399601 (97d:52034).

[LW97] J. C. Lagarias and Y. Wang, *Integral self-affine tiles in* $\mathbf{R}^n$. *II. Lattice tilings*, J. Fourier Anal. Appl. **3**(1) (1997), 83–102; MR 1428817 (98b:52026).

[MW88] R. D. Mauldin and S. C. Williams, *Hausdorff dimension in graph directed constructions*, Trans. Amer. Math. Soc. **309**(2) (1988), 811–829; MR 961615 (89i:28003).

[NN03] S.-M. Ngai and N. Nguyen, *The Heighway dragon revisited*, Discrete Comput. Geom. **29**(4) (2003), 603–623; MR 1976609 (2004d:28023).

[NT04] S.-M. Ngai and T.-M. Tang, *A technique in the topology of connected self-similar tiles*, Fractals **12**(4) (2004), 389–403; MR 2109984 (2006b:52018).

[NT05] S.-M. Ngai and T.-M. Tang, *Topology of connected self-similar tiles in the plane with disconnected interiors*, Topology Appl. **150**(1–3) (2005), 139–155; MR 2133675 (2006b:52019).

[Pra92] B. L. Praggastis, Markov partitions for hyperbolic toral automorphisms, Ph.D. thesis, University of Washington, ProQuest LLC, Ann Arbor, MI, 1992; MR 2687824.

[Rau82] G. Rauzy, *Nombres algébriques et substitutions*, Bull. Soc. Math. France **110**(2) (1982), 147–178; MR 667748 (84h:10074).

[Sin68] Ja. G. Sinaĭ, *Markov partitions and U-diffeomorphisms*, Funktsional. Anal. i Prilozhen. **2**(1) (1968), 64–89; MR 0233038 (38 #1361).

[Soc] J. Socolar, Tiling encyclopedia, http://tilings.math.uni-bielefeld.de/substitution/limhex.

[Sol97] B. Solomyak, *Dynamics of self-similar tilings*, Ergodic Theory Dynam. Systems **17**(3) (1997), 695–738; MR 1452190 (98f:52030).

[ST03] K. Scheicher and J. M. Thuswaldner, "*Neighbours of self-affine tiles in lattice tilings*", in *Fractals (Graz, 2001)*, Trends Math., Birkhäuser, Basel, 2003, 241–262. MR 2091708 (2005f:37039).

[Str93] R. S. Strichartz, *Wavelets and self-affine tilings*, Constr. Approx. **9**(2–3) (1993), 327–346; MR 1215776 (94f:42039).

[Thu89] W. Thurston, Groups, tilings, and finite state automata, AMS Colloquium Lecture Notes, Geometry Computing Group, 1989.

[Vin00] A. Vince, "*Digit tiling of Euclidean space*", in *Directions in Mathematical Quasicrystals*, CRM Monogr. Ser. **13**, American Mathematical Society, Providence, RI, 2000, 329–370. MR 1798999 (2002g:52025).

[Wan02] Y. Wang, *Wavelets, tiling, and spectral sets*, Duke Math. J. **114**(1) (2002), 43–57; MR 1915035 (2003e:42057).

Shigeki Akiyama
Institute of Mathematics
University of Tsukuba
1-1-1 Tennodai
Tsukuba
Ibaraki
Japan (zip:350-8571)
`akiyama@math.tsukuba.ac.jp`

Benoît Loridant
Lehrstuhl Mathematik und Statistik
Montanuniversität Leoben
Franz Josef Straße 18
A-8700 Leoben
Austria
`loridant@geometrie.tuwien.ac.at`